Université Abou Moumouni

Doctoral Research Program on Climate Change and Energy (DRP-CCE)

NIGER

INTERNATIONAL MASTER PROGRAM IN RENEWABLE ENERGY AND GREEN HYDROGEN

SPECIALITY:

ENERGY SYSTEMS ANALYSIS FOR GREEN HYDROGEN TECHNOLOGIES

MASTER THESIS

Topic:

TECHNO-ECONOMICAL OPTIMIZATION OF GREEN HYDROGEN PRODUCTION WITH RENEWABLE ENERGY SYSTEMS

Presented the 25 September 2023 and by:

Dayagnewendé Victorien OUEDRAOGO

Jury Members

Chairman: Prof. Rabani Adamou, University Abdou Moumouni

Examinator: Ass. Prof. Mounkaila Saley Moussa, University Abdou Moumouni

Supervisor from Germany: Pr. Andrea Benigni, Forschungszentrum Julich

Local Supervisors: Dr Inoussa Maarouhi, University Abdou Moumouni

Dr Boubacar Ibrahim, University Abdou Moumouni

Academic year 2022-2023

DEDICATIONS

First of all, I dedicate this work to Almighty God for all the graces, wisdom and strength that have been bestowed upon me throughout my life, particularly in completing my Master's studies.

To my dear parents and siblings, whose prayers have always accompanied my achievements and supported me in the difficult moments of my life.

To my dear fiancée for her prayers and invaluable support during my studies abroad.

To my friends and comrades at my formal institute, IFTSA of Joseph KI-ZERBO University and those from the IMP-EGH, who have contributed to my work and support me throughout my Master's studies.

ACKNOWLEDGEMENTS:

My sincere appreciation goes to the Federal Ministry of Education and Research (BMBF) and the West African Science Centre on Climate Change and Adapted Land Use (WASCAL) for providing the scholarship and financial support for this program.

I am thankful to the President of the University of Abdou Moumouni (UAM) and the staff for giving us the facility to study in a peaceful environment of this high place of education in Niger.

I would like to thank Prof. Andrea Benigni the Director of the Institute for Energy and Climate Research 10 (IEK 10) at the Jülich Research Centre (Forschungszentrum Jülich) and my supervisor for accepting us as members of the Institute and providing us with a very peaceful environment and facilities to work during our internship. Thanks for the assistance and guidance during the elaboration of my master's thesis and my stay in Germany

My sincere gratitude to the Director of WASCAL Niger and Rector of the University Abdou Moumouni, Prof. Rabani Adamou, who, apart from being our director, has been a senior for us early researchers and as a mentor through his advice to keep us in the right direction during our stay in Niamey.

My thanks to the Deputy Director Dr Inoussa Maarouhi one of my co-supervisors from Niger, the scientific coordinator Dr Moussa Mounkaila and the coordinator of H_2 Dr Ayouba Abdoulkadri for their commitment and availability in assisting us during our stay in Niamey for our Master's studies. My thanks are extended to Dr Boubacar Ibrahim my second co-supervisor from Niger for his assistance.

My thanks go towards the Jury's members composed by the president Prof. Rabani Adamou, the examinator Ass. Prof. Mounkaila Saley Moussa and my supervisors I Germany and in Niger.

I would also like to thank all the WASCAL staff, especially those involved in the green hydrogen program, Mr Hamidou Hama and his assistant Mr Alassane Fadel, Mr Moumouni and technical assistant Mr Agbo David for their commitment and efforts in facilitating our stay and studies at UAM. Not forgetting all our teachers for their various courses and advice.

My thanks are extended to our advisors Li Chuan and Yiwen Pan from the Institute for Energy and Climate Research 10 (IEK 10) at the Jülich Research Centre, who provided us with undeniable help and assistance, particularly in the modelling and thesis writing stages during our internship in Germany.

ABSTRACT

The future of the planet is at stake; for reasons, pollution of all kinds exacerbates the effects of climate change. Using renewable energy and energy carriers such as green hydrogen are advocated to be the most reliable solution. However, the technologies are still expensive and their performances are dependent on meteorological parameters making green hydrogen less cost-competitive. Depending on the location and the resources available, some renewable energy systems are more suitable to provide hydrogen at lower prices. Therefore, it is necessary to build a techno-economical optimization model that determines among several sets of renewable energy systems (Land PV, floating PV and hybrid land PV-Wind and floating PV-Wind) and electrolyser technologies (Alkaline electrolyzer, proton exchange membrane electrolyser and solid oxide electrolysis cells), the optimal configuration that gives a lower levelized cost of hydrogen. To achieve this goal, we use the COMANDO energy system optimization framework (ESOF) within which we have modelled the components and the energy and formulated optimization problem. With the Gurobi optimizer, we got the optimal results which are used to calculate the levelized cost of hydrogen and perform the sensitivity analysis. The results show that the land PV coupled with alkaline electrolyser gives the lowest cost of hydrogen with 5.926€/kgH_2 followed by the floating photovoltaic coupled with alkaline electrolyser with 6.038€/kgH_2. By selling the oxygen produced at 0.5€/kgO_2, the levelized cost of hydrogen could drop by 41.4% to 66.2% depending on the energy system reaching 2.02€/kgH_2 to 5.62€/kgH_2. The carbone emission per kilogram of hydrogen produced ranged between 24.17 to 34.07 g/kgH_2 which is far below the threshold set to 1kgCO_2/kgH_2 by the Green Hydrogen Organisation. Furthermore, for the floating photovoltaic, the water savings from evaporation is evaluated to be around 6.08 to 8.506 million cubic meters per year. The sensitivity analysis shows that among the parameters, the discount rate, the electrolyser efficiency and the total installed costs of the components are more impactful on the cost of hydrogen. Notwithstanding the details considered in this study, other aspects could be considered in the modelling such as the integration of the alternative direct current power network as well as the hydrogen flow network. The accuracy and updated costs could be the subject of further investigations to get more accurate results.

Key words: Green hydrogen; Floating PV; ESOF; COMANDO; Gurobi, LCOE, LCOH

RÉSUMÉ

L'avenir de la planète est en jeu ; pour des raisons de pollutions de toutes sortes qui exacerbent les effets du changement climatique. L'utilisation d'énergies renouvelables et de vecteurs énergétiques tels que l'hydrogène vert est préconisé comme la solution la plus fiable. Cependant, les technologies sont encore coûteuses et leurs performances dépendent des paramètres météorologiques, ce qui rend l'hydrogène vert moins compétitif sur le plan des coûts. Cependant, en fonction de l'emplacement et des ressources disponibles, certains systèmes d'énergie renouvelable sont plus appropriés pour fournir de l'hydrogène à moindre coût. Par conséquent, il est nécessaire de développer un modèle d'optimisation technico-économique qui détermine parmi plusieurs ensembles de systèmes d'énergie renouvelable (PV terrestre, PV flottant et hybride PV-éolien terrestre et PV-éolien flottant) et de technologies d'électrolyseurs (Électrolyseur alcalin, électrolyseur à membrane échangeuse de protons et cellules d'électrolyse à oxyde solide), la configuration optimale donnant un coût actualisé bas de l'hydrogène. Pour atteindre cet objectif, nous avons utilisé le cadre d'optimisation des systèmes d'énergie (COSE) COMANDO dans lequel nous avons modélisé les composants, les systèmes énergétiques et formulé le problème d'optimisation. Avec l'optimiseur Gurobi, nous avons obtenu les résultats optimaux qui sont utilisés pour calculer le coût actualisé de l'hydrogène et effectuer l'analyse de sensibilité. Les résultats montrent que le photovoltaïque terrestre couplé à un électrolyseur alcalin donne le coût le plus bas de l'hydrogène avec 5.926€/kgH_2 suivi du photovoltaïque flottant couplé à un électrolyseur alcalin avec 6.038€/kgH_2. En vendant l'oxygène produit à 0,5€/kgO_2, le coût actualisé de l'hydrogène pourrait baisser de 41,4% à 66,2% selon le système énergétique atteignant 2,02€/kgH_2 à 5,62€/kgH_2. Les émissions de carbone par kilogramme d'hydrogène produit se situent entre 24,17 et 34,07 g/kgH_2, ce qui est bien inférieur au seuil fixé à 1 kgCO_2/kgH_2 par l'Organisation de l'Hydrogène Vert. En outre, pour le photovoltaïque flottant, les économies d'eau dues à l'évaporation sont évaluées à environ 6,08 à 8,506 millions de mètres cubes par an. L'analyse de sensibilité montre que parmi les paramètres, le taux d'actualisation, le rendement de l'électrolyseur et les coûts totaux d'installation des composants ont plus d'impact sur le coût de l'hydrogène. Nonobstant les détails pris en compte dans cette étude, d'autres aspects pourraient être pris en compte dans la modélisation tels que l'intégration du réseau d'alimentation à courant alternatif et continue ainsi que le réseau de flux d'hydrogène. La précision et l'actualisation des coûts pourraient faire l'objet d'études plus approfondies pour obtenir des résultats plus précis.

Mots clés : Hydrogène vert ; PV flottant ; COSE ; COMANDO ; Gurobi

ABBREVIATIONS AND ACRONYMS

AEL: Alkaline Electrolyser

BOS: Balance of plant

BMBF: Bundesministerium für Bildung und Forschung (Federal Ministry of Education and Research)

CapEx: Capital Expenditures

CCUS: Carbone Capture, Utilisation and Storage

CO_2: Carbone dioxide

COMANDO: Components-oriented modelling and optimisation for Non-linear Design and Operation

ES: Energy System

ESOF: Energy Systems Optimization Framework

FPV: Floating photovoltaic

F_{PV}A: Floating photovoltaic with alkaline electrolyser

F_{PV}P: Floating photovoltaic with proton exchange membrane electrolyser

F_{PV}S: Floating photovoltaic with a solid oxide electrolysis cell

F_{PV}WA: Floating photovoltaic and wind with an alkaline electrolyser

F_{PV}WP: Floating photovoltaic and wind with proton exchange membrane electrolyser

F_{PV}WS: Floating photovoltaic and wind with a solid oxide electrolysis cell

F_{PV}WS: Land photovoltaic and wind with a solid oxide electrolysis cell

GHGs: Greenhouse gas

GSA: Global Sensitivity Analysis

H_2: Hydrogen molecule

HDPE: High-Density Poly-Ethylene

IFTSA : Institut de Formation en Technologies Solaires Appliquées

IMP-EGH: International Master Program in Energy and Green Hydrogen

KOH: Potassium hydroxide

LCOE: Levelized cost of electricity

LCOH: Levelized cost of hydrogen

LCOO: Levelized cost of oxygen

LPV: Land photovoltaic

$L_{PV}A$: Land photovoltaic with an alkaline electrolyser

$L_{PV}P$: Land photovoltaic with proton exchange membrane electrolyser

$L_{PV}S$: Land photovoltaic with a solid oxide electrolysis cell

$L_{PV}WA$: Land photovoltaic and wind with an alkaline electrolyser

$L_{PV}WP$: Land photovoltaic and wind with proton exchange membrane electrolyser

LSA: Local Sensitivity Analysis

MEA: Membrane electrode assembly

O_2: Dioxide

OAT: One-at-a-Time

OpEx: Operational Expenditures

PEME: Proton Exchange Membrane Electrolyzer

PV: Photovoltaic

R&D: Research and Development

RES: Renewable energy resources

RES: Renewable Energy sources

SO: Systems Operators

SOEC: Solid Oxide electrolysis cell

TACs: Total annualised costs

TICs: Total installed costs

WASCAL: West African Science Service Centre on Climate change and Adapted Land Use

Units

€: Euro

°C: Degree Celsius

CNY: Chinese Yuan

EUR: Euros

GW: Gigawatt

GWh: Gigawatt-hour

INR: Indian Rupee

kg: Kilogram

kgH_2: Kilogram of hydrogen

km: kilometres

kWh: kilowatt-hour

m^2: Square meter

MW: Megawatt

TWh: Terawatt hour

USD: United States Dollar

W: Watt

Wp: Watt-peak

LIST OF TABLES

LIST OF FIGURES

TABLE OF CONTENTS

1 Introduction

The current state of the world's climate is a cause of concern for everyone. The planet is getting warmer and warmer due to the high concentration of greenhouse gases (GHGs) in the atmosphere. The observed high concentration of GHGs is undeniably due to human activity emissions which contribute to a warming of 1.0 ℃ to 2 ℃ (IPCC-AR6, 2023). This situation is alerting all the countries on their energy supply and used systems. Countries having high emission rates are urging to adopt strategies and policies that foster emissions reduction and decarbonization of their sectors as the objective is to limit the average global surface temperature increase below 2℃ according to the Paris Agreement (UNFCCC, 2016). It is crucial to control GHGs from energy production and consumption to be capable of combating climate change (Osman et al., 2022). Among the solutions found to achieve net-zero emissions and more sustainability, the most promising is using renewable energy sources (RES). (RES) are known as inexhaustible energy sources that continuously supply clean energy (National Geographic Society, 2023). Renewable growth is a key pillar for the energy transition. The energy transition process implies integrating renewable energy in the energy-intense and high-emitting sectors such as the hard-to-abate sectors (IEA, 2019; Singlitico et al., 2021). In other words, even though renewable energy is cost-effective (varies by location), transporting it over long distances becomes less cost-effective (IEA, 2019). An energy carrier is required to achieve a considerable integration of renewable energy into the end-use sectors via sector coupling. Green hydrogen appears to be an attractive energy carrier as it facilitates large amounts of RES to be directed from power systems into the end-use sectors such as transport, building and industries. Besides being a reliable energy carrier, green hydrogen has been identified as one of the most promising options for long-duration electricity storage (Rabiee et al., 2021). According to the Green Hydrogen Standard defined by the Green Hydrogen Organization, hydrogen is qualified green if it is produced through the electrolysis of water using renewable energy (Green Hydrogen Organization, 2022).

However, despite the high advancement in the field of renewable technologies, green hydrogen is still expensive. This is due to several factors including the high costs of green hydrogen production utilities, the high cost of renewable electricity and the expensive access to sustainable water. Investments in fixed assets, power generation and operation expenses such as water preparation and consumption represent most of the costs of water-electrolytic hydrogen production (Hassan et al., 2023). Moreover, the electricity output and the efficiency

of the solar photovoltaic (PV) modules are highly dependent on some weather factors such as solar irradiation and ambient temperature as low irradiation and or high ambient temperature dramatically decrease the PV modules' output (Bonkaney et al., 2017; Dewi et al., 2019; Dubey et al., 2013; Sachenko et al., 2020; Skoplaki & Palyvos, 2009), therefore affecting the cost of electricity produced. In addition, the integration of variable renewable sources such as wind and solar energy known for their intermittency, imposes unavoidably additional flexibility requirements on Systems Operators (SO) for them to guarantee an instantaneous equilibrium between supply and demand. These flexibility requirements imply additional costs impacting highly also the electricity cost (Batalla-Bejerano & Trujillo-Baute, 2016). Green hydrogen becomes less competitive with the other types of hydrogen. For instance, hydrogen from natural gas and coal with carbon capture sequestration cost 1.2-2.1 USD/ kgH_2 and 2.1-2.6 USD/kgH_2 respectively in 2019 while hydrogen from renewables-based energy cost 3.2-7.7 USD/ kgH_2 (IEA, 2020). Even though green hydrogen is a carbon-neutral energy, one can conclude that green hydrogen is less attractive and less cost-effective for any sector and more for energy-intense sectors.

Knowing the key factors that make green hydrogen so expensive, it is very crucial and necessary to investigate the potential approaches that could considerably reduce the cost of green hydrogen and make it cost-competitive. Some studies show that green hydrogen's cost competitiveness depends on the application sector, the availability of renewable energy and water resources and space for implementation (Hydrogen Council, 2020; Woods et al., 2022). However, most of the regions with huge renewable energy resources and space are the most vulnerable in terms of water scarcity (Woods et al., 2022); that is the case in Australia and the Sahelian and northern parts of Africa.

In this context, this work aims to investigate the techno-economics of renewable electricity and green hydrogen production using different configurations of renewable technologies (Land PV, floating PV and hybrid land PV-Wind and floating PV-Wind) combined with different electrolyser technologies (Alkaline electrolyzer, proton exchange membrane electrolyser and solid oxide electrolysis cells) taking into account key factors such as weather factors and availability of water.

1.1 Problem analysis and motivation

To protect the planet and achieve sustainable development, many countries are committed to combating climate change. One of the most appropriate ways to achieve this goal is to switch from fossil fuels to renewable energies. Using hydrogen and its derivatives

as energy carriers to ensure energy integration and sector coupling proves to be worthy mostly for hard-to-abate sectors. However, green hydrogen production faces several challenges as it is highly dependent on important factors such as the renewables potentials known as very intermittent, the renewables' technology costs, the water accessibility which is very crucial for hydrogen production and some weather factors such as temperature that impact the PV output. These factors influence more or less the costs of renewable energy and green hydrogen. As mentioned in many reports, hydrogen is expected to contribute up to 10% of the CO_2 emission reduction in 2050 and fulfil 12% of the global energy demand (IRENA, 2022a) and even 18% of the global energy by 2050 (Hydrogen Council, 2020). This implies unavoidably hydrogen cost reduction to at least 2.60 USD/kgH_2 to reach cost parity (Hydrogen Council, 2020). To achieve this objective, it is vital to identify suitable locations and energy system configurations for green hydrogen production, making the best possible assessment of the technical and economic aspects.

Many authors have undertaken techno-economic assessments of hydrogen production and hydrogen cost reduction analyses for specific locations. Their results cannot therefore be applied everywhere, as the economic parameters, cost assumptions, resource availability and component lifetimes differ from one place to another and from one author to another and are even subject to local factors.

This study aims to design a techno-economic optimization model that minimizes the green hydrogen production costs by optimizing the capacities of the renewable energy systems and the green hydrogen production plant and the investment costs. By doing so, we are presenting pragmatic results that can help and support decision-makers' and stakeholders' decisions. The method is to explore the energy system configurations combining land photovoltaic (LPV), floating photovoltaic (FPV), and onshore wind power to whether an alkaline electrolyzer (AEL), a proton exchange membrane electrolyzer (PEME) or a solid oxide electrolysis cell (SOEC) and to identify the optimal configuration that gives a lower levelized cost of hydrogen (LCOH). An energy system optimization framework (ESOF) called COMANDO developed by the Institute of Energy and Climate Research 10 (IEK 10) of the Research Centre Jülich is used. The model built could be applied to any location by only inputting the data of the chosen location.

1.2 Research questions

1.2.1 Main research question

What is the appropriate energy system for green hydrogen production, taking into account weather conditions and water availability, and how can it be optimized to reduce LCOH?

1.2.2 Research sub-questions

To address this main research question in our work, we will proceed by answering the below sub-questions.

- What are the most widely used mature renewable energy systems for green hydrogen production?
- What are the main meteorological parameters that influence the efficiency and yield of a solar photovoltaic system?
- What impact does the water-cooling effect have on the yield of a floating photovoltaic system?
- What are the efficiency and yield of the FPV system compared to the LPV system?
- What is the impact of water accessibility on the hydrogen cost?
- What configuration of the energy system would be best for reducing the cost of electricity and hydrogen?
- What are the optimum capacities and costs of the components of the green hydrogen production plant?
- What are the levelized cost of electricity (LCOE) and the levelized cost of hydrogen (LCOH)?
- What is the impact of the lifetime, cost, demand and nominal discount rate variations on the optimum capacities and investment costs?
- What is the carbon footprint of the hydrogen produced by the green hydrogen production plant?

1.2.3 Research hypotheses

Our expectations from the results are as follow:

- The efficiency and yield of the floating photovoltaic system could be slightly higher than those of the LPV system due to the water-cooling effect.
- The LOCE of the floating PV could get lower due to the water-cooling effect which could slightly increase the yield.

- The LCOH could be lower for floating PV compared to the LPV due to the proximity of the water.

1.2.4 Research objectives

The ultimate objective of this work is to design a flexible techno-economical optimization model of green hydrogen production using renewable energy systems such as solar and wind. This model could be applied anywhere in the world to assess the technical and economic aspects of green hydrogen production. For this study, we will take Ghana as a case study and more specifically the water reservoir of Akosombo's dam for the floating PV and Bonkoko located 57 km from Akosombo for the LPV. The production of green hydrogen requires the accessibility and availability of sustainable water. To not impact negatively the water access to the population, we chose a location with low water scarcity which is Ghana particularly the Akosombo dam water reservoir. To achieve the main objective, we will gradually fulfil these specific objectives mentioned below:

- Identify the most used renewable resources for electricity and green hydrogen
- Identify the main meteorological factors that can impact the yield of a solar PV plant.
- Assess the impact of the cooling effect on the solar PV plant.
- Undertake a comparative analysis of performance between FPV and LPV.
- Determine the optimal energy system configuration, its optimum capacities and investment costs.
- Evaluate the LCOE and the LCOH
- Discuss the impact of water accessibility on the hydrogen cost
- Undertake a sensitivity analysis of the optimized systems with variations of the lifetime, cost, efficiencies and nominal discount rate.
- Evaluate the carbon footprint of the green hydrogen produced.

1.2.5 Announcement of the plan

This work is divided into an introduction, 3 main chapters and a conclusion presented according to the following outline:

- The introduction introduces the overall context, the justification of the study mentions the problem statement, the research questions, the research hypothesis and the research objectives and finally the announcement of the outline.
- Chapter one contains the literature review that presents the main results of other research in the techno-economic assessment of green hydrogen production.

- Chapter two describes the methodology and modelling steps used to design the techno-economic optimization model. It shows also how the data and parameters are collected and processed for the case study of Akosombo and Bonkoko.
- Chapter three presents the optimized results of the model and discussion
- Conclusions of the current study and perspectives relative to the current and further research.

2 Literature Review

2.1 The global state of renewable energy generation and trends

Renewable energy resources are standardly defined as natural inexhaustible energy sources that continuously supply clean energy (National Geographic Society, 2023). Compared with fossil fuels, renewable energy resources are available and exploitable on a viable scale throughout the world (IRENA, 2022a), particularly solar and/or wind power. However, they are not evenly distributed across the globe. To achieve their goals towards the Paris Agreement (UNFCCC, 2016), most countries are committed to accelerating the energy transition by exploiting as much as possible the renewable energy resources available in their territory. Across the world, renewable energy projects mostly solar and wind projects are developed to increase renewable electricity production to meet the energy demand while aiming for net-zero carbon emissions.

According to the International Energy Agency, the global cumulative PV capacity is expected to reach 2,350 GW by 2027 becoming the largest installed electricity capacity worldwide. The overall electricity generation is expected to increase by around 60% reaching over 12,400TWh led by hydropower followed by wind and solar PV. At the regional level, China is ahead and expects to reach 1,070 GW of cumulative renewable power capacity by 2027, with solar PV and wind accounting for 90% of renewable energy growth. China also ambitions to achieve its 2030 target of 1200 GW of total wind and solar PV capacity five years earlier (IEA, 2022b). The United States is forecasting an increase of 75% or over 280 GW of renewable energy capacity from 2022 to 2027 with solar PV and wind accounting for almost all the renewable expansion (IEA, 2022b). In Europe, the renewable energy expansion is concentrated in seven countries (Germany, Spain, the United Kingdom, Türkiye, France, the Netherlands and Poland) and is expected to increase by around 60% (425GW additional) (IEA, 2022b). This growth is led by solar PV followed by wind. In the Asia Pacific region excluding China, solar PV accounts for more than two-thirds of the expected expansion

followed by wind and hydropower. The renewable capacity is forecasted to grow by 360 GW (more than 70%) from 2022 to 2027 (IEA, 2022b). Renewable power capacity in Latin America is expected to increase 45% (+130 GW) during 2022-2027 with solar and wind counting 90% of the region's expansion (IEA, 2022b). In the Middle East and North Africa, the expansion is expected to triple by 2027, reaching 45 GW. Due to attractive economics for utility-scale projects, significant solar resource potential and favourable financing conditions, solar PV constitutes three-fourths of the capacity growth in this region (IEA, 2022b). In the case of Sub-Saharan Africa, the capacity of renewable power is forecasted to double with more than 40 GW additional by 2027. Solar PV and wind lead the capacity growth and account for over 60% of the overall capacity additions (IEA, 2022b).

The increasing trend of renewable energy capacities across the world can be explained by the necessity to decarbonize high-emitting sectors by integrating renewables through energy carriers such as green hydrogen and its derivatives. This can be done by using power-to-X (e.g., power-to-hydrogen, power-to-ammonia) processes. As a matter of fact, in 2021, water electrolysis represented only 0.1% of the overall hydrogen production, but by the end of 2021, the capacity of the electrolyser was expected to reach 510 MW approximately 70% relative to 2020 (IEA, 2022a). In addition, more than 4 Mt of electrolytic hydrogen is expected to be produced in Africa, Latin America and the Middle East by 2030 (IEA, 2022a).

2.2 Overview of green hydrogen production systems

Renewable electricity can be subject to curtailments due to its challenging integration into sectors such as industry, mobility, domestic and commercial sectors. The Power-to-Gas approach is identified to be one of the promising solutions to assure inter-sectoral coupling (Gorre et al., 2020a). Power-to-gas is a technology that uses renewable electricity flexibly to produce hydrogen (H2) qualified as green, by water electrolysis. Water electrolysis is an electrochemical reaction during which the water is split into hydrogen and oxygen thanks to the electricity and/or heat supplied (Buttler & Spliethoff, 2018).

$$H_2O \xrightarrow{Electrolysis} H_2 + \frac{1}{2}O_2 \qquad 2.2\text{-}1$$

To date, two major technologies are used to process water electrolysis: alkaline electrolyzer (AEL) and proton exchange membrane electrolyzer (PEME); other emerging technologies such as solid oxide electrolyzer (SOEL) and anion exchange membranes electrolyzer (AEME) are yet to be developed and deployed (Buttler & Spliethoff, 2018; IEA, 2022a).

2.3 Renewable electricity and Green Hydrogen production costs.

The renewable resources' potential is regional dependent; in other words, from one location to another, the renewable resources vary. This variation drives the cost of renewable electricity and directly the cost of the renewable hydrogen produced from this electricity. In the literature, many authors undertook technical and economic assessments of green hydrogen in different locations in the world, to determine how feasible and cost-effective a renewable electricity and/ or green hydrogen production project is in those areas. Different approaches and configurations have been consideredt.

Gurfude et al. (2020) undertook a techno-economic analysis of a one-megawatt peak of FPV at Ambazari Lake, Nagpur, state Maharashtra, India and found a LCOE of 3.096 INR/kWh (0.036 €/kWh, 2020 exchange rate). Goswami et al. (2019) compared a FPV to a LPV in a techno-economic analysis and found USD0.026/kWh and USD0.042/kWh respectively. Gonzalez Sanchez et al. (2021) assessed the FPV potentials in existing hydropower reservoirs in Africa. They found LCOE of 0.022€/kWh and 0.035€/kWh respectively for the FPV and LPV.

Regarding the cost of green hydrogen, several authors investigate its production using different renewable energy systems. Terlouw et al. (2022) evaluated a techno-economic and environmental assessment of a large-scale hydrogen production plant via electrolysis and found that with an off-grid PV, they achieved a LCOH of 9.6–17.2 €/kgH_2. With an off-grid PV energy system, Hassan et al. (2023) concluded that depending on the technology used, the LCOH can vary between USD3.23-5.39/kgH_2 (2.974-4.96€/kgH_2, 2023 exchange rate). With a hybrid PV-Wind energy system, Woods et al. (2022) determined the LCOH and found value ranged between $4 to $6/kg$H_2$ (3.804-5.706€/kgH_2, 2022 exchange rate). Khan et al. (2021) compared the costs of hydrogen produced from silicon-based PV and concentrator PV. They found respectively $4.9/kg$H_2$ and $5.9/skg$H_2$ for the silicon-based PV and the contractor PV. Gökçek & Kale (2018) considered a hybrid PV-Wind and a wind power energy system. By comparing the cost of the hydrogen produced by those systems, they found $6.92/kg$H_2$ for the hybrid system and $9.09/kg$H_2$ for the wind power energy system. Shaner et al. (2016) perform a comparative techno-economic analysis of green hydrogen production using solar energy. They found that with the PV energy system, the LCOH is around $12.1/ kg$H_2$. According to the global hydrogen review of IEA (2022a), the cost of hydrogen produced by renewable energy ranges between USD4.0-9.0/kgH_2.

According to the International Renewable Energy Agency, at a global scale the tendency of the global weighted LCOE of renewable electricity more specifically wind and solar, is downwards from 2020-2021. In 2021, the utility-scale solar PV and offshore wind LCOE saw a decline of 13% while the onshore wind is 15%. This results in a year-on-year decline from USD0.055/kWh to USD0.048/kWh for solar PV, from USD0.039/kWh in 2020 to USD0.033/kWh for onshore wind and from USD0.086/kWh to USD0.075/kWh for offshore wind. The rapid fall in total installation costs, the increase in capacity factors and the reduction in operating and maintenance costs have all contributed to a remarkable reduction in the cost of solar photovoltaic and wind electricity and an improvement in their economic competitiveness (IRENA, 2022b).

The International Energy Agency projects the hydrogen cost to fall due to the improvement of the technologies, the reduction of the total investment cost of the renewable technologies, and their deployment. This will highly impact the cost-effectiveness and the competitiveness of green hydrogen regarding hydrogen production from natural gas with CCUS (Carbone Capture, Utilisation and Storage). In regions with good solar conditions, green hydrogen from solar PV could fall below USD1.5/kgH_2 by 2030 and by 2050 below USD1/kgH_2. This could be possible if only the costs of electricity from solar PV (representing 55% of hydrogen production costs) fall to USD14/MWh by 2030 and USD11/MWh by 2050. The global potential of offshore wind could provide a green hydrogen cost below USD3/kgH_2 by 2030 (IEA, 2022a). According to the hydrogen council, if the CapEx of the full electrolysis system decreases driven by large deployment in production, learning rate, and technological improvements, the cost of hydrogen produced could drop from USD2/kgH_2 to USD0.50/kgH_2 by 2030 (Hydrogen Council, 2020).

2.4 Key meteorological parameters influencing the PV performance

2.4.1 Temperature and wind effect on PV performance

A solar PV system is a generator that produces electricity thanks to the PV modules that convert solar radiation into electricity. Studies carried out by some authors concluded that photovoltaic modules' efficiency is temperature dependent as the efficiency drops when the module temperature increases. Bonkaney et al. (2017) found that under Sahelian climate conditions, with each degree Celsius of ambient temperature rise, the output of the PV module decreases by 2.6% whereas the efficiency drops by 0.49%. His result is in line with the values given by other authors in Skoplaki & Palyvos (2009)'s review. Bouraiou et al. (2015) conducted a study on the impact of desert climate conditions on the PV performance namely

the temperature and the dust accumulation. He observed a loss of the maximum power output on the two modules used: the first module's loss was 28.62% with a 2.6%/year degradation rate and the second module's loss was 12.99% and 1.18%/year degradation rate. Leow et al. (2019) undertook a practical experiment to determine the influence of wind speed on the performance of photovoltaic panels. Comparing the output of a PV module exposed to the wind with another without wind flow, he found that a non-exposed PV module to wind speed generated an average output power of 42.42 W with an average operating temperature of 53.7°C. Whereas, the PV module with wind generated an average output power of 49.47 W with an average operating temperature of 49.5 °C. His study proves that wind speed can improve the solar PV module's output by up to 14.25 % because of the decrease in the operating temperature. Schwingshackl et al. (2013) came to the same conclusion that including wind speed in the cell temperature calculation with a model provides better and more accurate results.

2.4.2 Water cooling effect on PV performance and water savings

The water-cooling effect is a consequence of thermal interactions between the above air temperature and the water temperature. One can notice that the air temperature near or over water bodies can be significantly different from that over land or on rooftops. This can be explained by several mechanisms. The first mechanism is that water is transparent, which means that the energy from incoming solar radiation is not just transmitted to the surface layer, unlike on land. As a result, the surface of the water, which interacts with the photovoltaic module, remains cooler. A second mechanism is that compared to land PV where most irradiation heats the surrounding environment; a large proportion of the irradiation evaporates the water for floating PV. A third mechanism is that water can circulate freely. Surface water warmed by incoming solar radiation can mix with colder water at greater depths, which is not the case for land PV systems (Dörenkämper et al., 2021). In conclusion, since the ambient temperature above water gets lower compared to the ambient temperature above land, it is expected that PV modules have cooler temperatures.

Many authors investigated the impact of the water-cooling effect on the operating cell temperature, the efficiency and the energy yield of PV modules. Dörenkämper et al. (2021) compared two floating PV systems installed in two different locations Netherlands and Singapore to the land-PV or rooftop-based PV benchmarks. It has been found that the best-performing floating PV systems showed 3.2 ◦C and 14.5 ◦C lower operating cell temperatures in Netherlands and Singapore respectively. In addition, the gain in energy yield from the

cooling effect of floating PV systems is up to 3% in the Netherlands and up to 6% in Singapore. Kjeldstad et al. (2021) compared two floating PV module strings, one in direct contact with the membrane resting on the water and another resting on a mounting structure. He observed that the first one exhibits a 5-7% higher yield than the second one. For him the floating PV technologies which are in direct contact with the water or very close to it, the water temperature constitutes their ambient temperature. Yadav et al. (2017) findings are also in line with the other authors. With two identical 250Wp PV modules, one installed overland and the other one over water, the maximum power output and efficiency were 166.95W, 11.63% and 168.83W, 12.42% respectively. This means that the floating PV system power output and efficiency values are increased up to 2.24% and 0.79% respectively (Yadav et al., 2017). Divya Mittal et al. (2017) found that floating PV systems have a 2.48% increment in annual energy with a 14.56% decrement in module temperature. Liu et al. (2017)'s results show that under similar ambient conditions, the cell efficiency of land PV cells is 14.35 % while for floating PV cells the efficiency is 14.59% which corresponds to an increase of 1.58-2.00 % for floating PV. Sahu et al. (2016) studies result in 11% higher efficiency for the floating PV plant compared to the land-based solar PV plant and a reduction of water evaporation by 70%. According to Gurfude et al. (2020) the efficiency of the Floating PV plant could be 2.5-3% more than the ground-mounted PV plant and save 191 million Liters of water annually from evaporation.

All the findings from the authors indicate that FPV undoubtedly increases the power output when compared to land PV.

2.5 Oxygen sales opportunities

Oxygen is a by-product of the water electrolysis process. In most of the techno-economic studies, it is not considered. However, oxygen is essential in some domains such as wastewater treatment, fuel cell operation, medical use, etc.

For the water treatment, the high purity of the oxygen released during the electrolysis process will be an asset leading to more oxygen solubilised in the digesters and will serve to produce ozone for further disinfection of the treated water (Woods et al., 2022). The oxygen could also be very relevant for hydrogen fuel cells that require, particularly pure oxygen. In the case of healthcare, pure oxygen appears to be very precious for hospitals. After conducting economic analysis for an oxygen production plant via electrolysis for hospitals, Squadrito et al. (2018) concluded producing oxygen on-site is much more economically profitable than purchasing it from local gas sellers.

Based on these reasons, collaboration with the oxygen end users can give an important sales opportunity for the oxygen produced that could be simply released into the atmosphere. This sales opportunity can amortize the green hydrogen cost and make it more affordable.

3 Methodology, description and modelling of green hydrogen production systems

3.1 Methodology structure

This study aims to design a techno-economic optimization model that minimizes the green hydrogen production cost by optimizing the capacity of the green hydrogen production plant and the investment costs. The approach adopted in this study consists first of all of choosing the location based on various criteria, such as the type of system wished to install (ground-mounted PV, floating PV, hybrid PV-wind ...), the land requirement for land PV, the water accessibility for the hydrogen production, the potential of the renewable sources ... The second step is to collect analyse and process the required data and parameters for the chosen system. Thirdly, the components of the energy system are modelled and used to configure the different energy systems. After, the optimization problem is formulated and solved using the Gurobi solver. The results obtained for the solving are analysed and used to do the techno-economic assessment by determining the LCOE and LCOH. We used the Python programming language for all the coding and computation parts of our work. Figure *3.1-1* shows the structure of the methodology. The first step consists of choosing the area where the study will be undertaken. After what the required data and parameters are collected, analysed and processed. In the second step, the energy systems and their components are modelled within the COMANDO framework. The next step consists of formulating and solving the optimization problem. After getting the optimal results, we proceed by assessing the CO2 emissions, the economics, the water proximity impact and the sensitivity analysis.

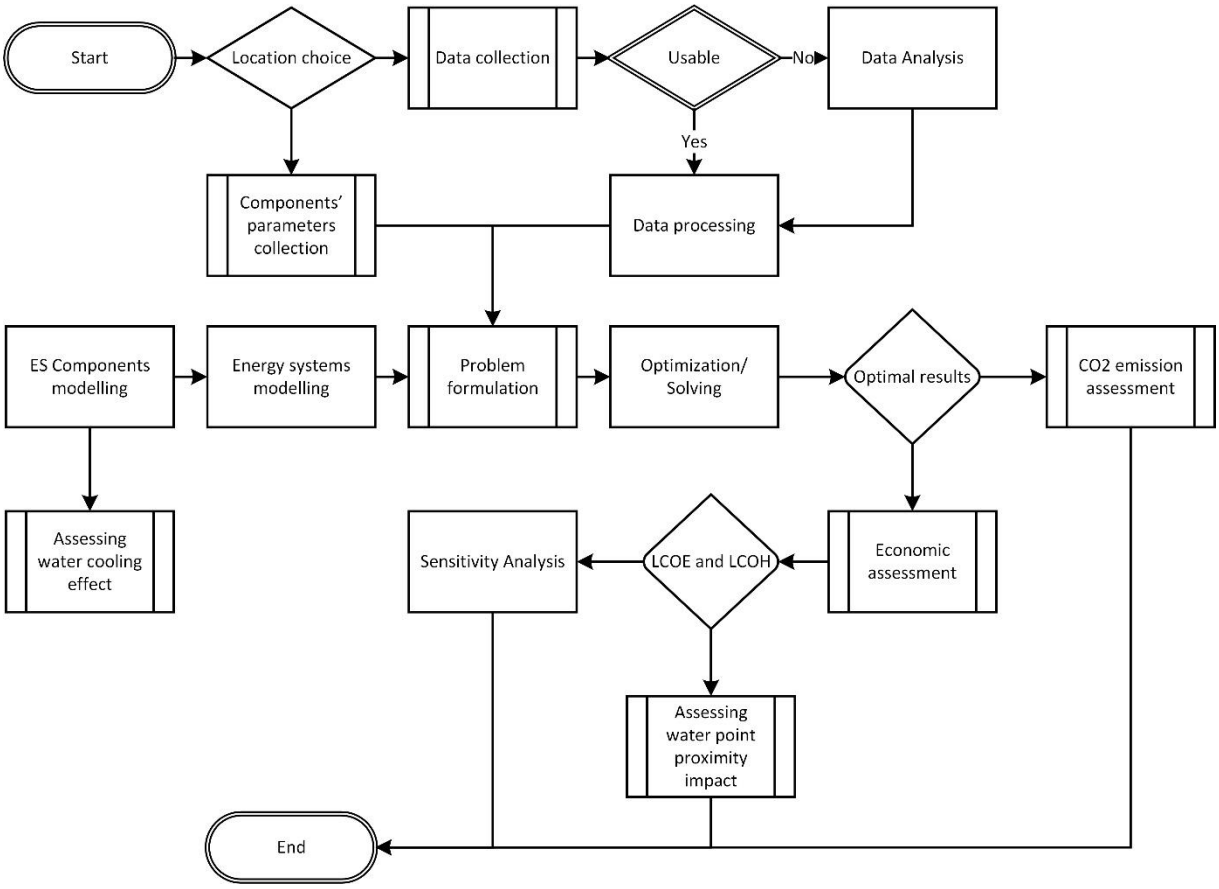

Figure 3.1-1: Methodology structure

3.2 The study areas

In this study, we will consider two areas, one favourable to floating PV implementation: Akosombo Dam water reservoir and another one for the land PV Bonkoko. In both cases, we will include an option to hybrid the indicated solar PV systems to wind power. These two locations are all in the Volta basin where water scarcity is relatively low. Therefore, they have been considered case study neglect constraints on water scarcity. Additionally, we assumed that both systems in Akosombo and Bonkoko have the same water access point which is Akosombo Dam downstream water.

Akosombo Dam is a hydroelectric dam built on the course of the Volta River. Its construction from 1961 to 1965 led to the formation of the Volta Lake, the largest man-made water reservoir in the world by surface area (8,480 km^2) and the world's third-largest by volume approximately 150 billion m^3 (Osei et al., 2019). The Volta-Lake is located at the latitude 6.489955° and longitude -0.000041°. The location near the equation, the large surface area and the huge reservoir capacity make the Akosombo Dam water reservoir a potential location for green hydrogen production using floating PV and wind power energy systems.

Bonkoko is a locality, a village situated within the same region as Akosombo Dam at the coordinate's latitude 6.287999°, and longitude -0.218079°. The village is 40 km from the Akosombo Dam Reservoir. Akosombo Dam and Bonkoko are on the same latitude, therefore, we can assume that their wind and solar potential are similar.

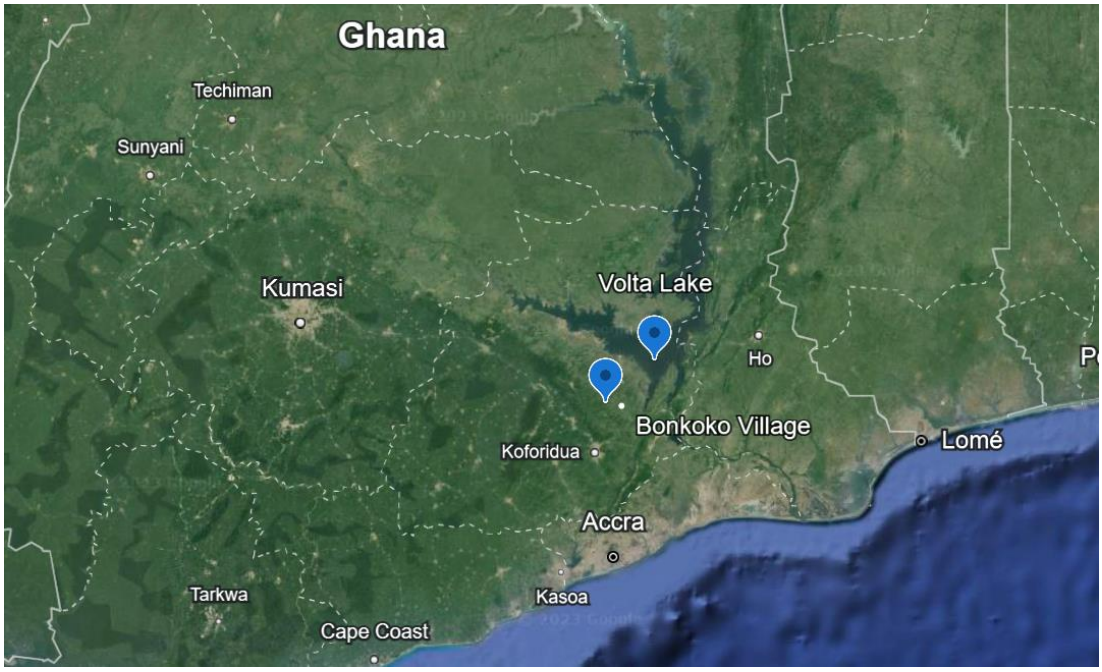

Figure 3.2-1: Location of sites for floating PV on the Volta Lake and land PV at Bonkoko Village.
(Google Earth, 2023)

Volta Lake and Bonkoko are geographically well-positioned to receive important solar irradiation due to their proximity to the equator. The global solar horizontal irradiation is 1853.1 kWh/m2 per year (GSA, 2023a) and 1937.1 kWh/m2 per year (GSA, 2023b) respectively for Bonkoko and Volta Lake. The Figure 3.2-2 below, represents the hourly solar radiation at the year 2019 of Bonkoko village. On this figure, we can notice that the maximum value of the hourly solar radiation is around 960 W/m^2. The solar potential observed is considerable for solar PV system implementation.

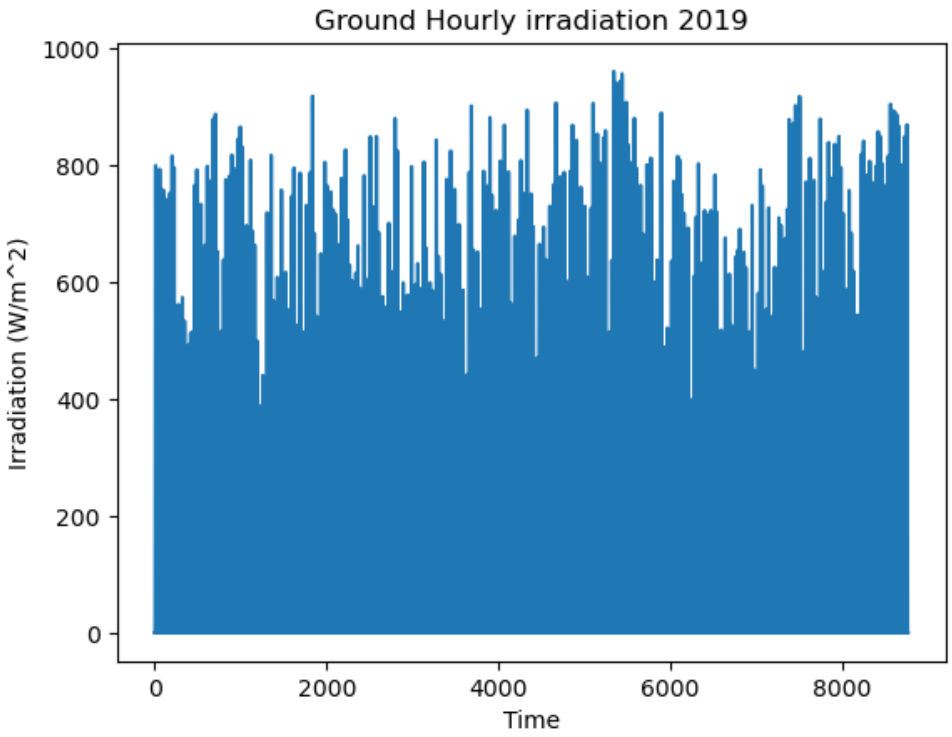

Figure 3.2-2: Hourly irradiation of Bonkoko village for the year 2019 (Stefan & Iain, 2023)

Regarding the wind potential, Bonkoko has an altitude of around 498 m, which gives it a high wind potential. As a matter of fact, at 100 m and 150 m height, the average wind speed and wind power density are around 7.43m/s, 381 W/m^2 and 7.83 m/s, 445 W/m² respectively (GWA, 2023b). In the case of Akosombo Dam, we will consider a wind farm installed not on the Volta Lake but next to the hydroelectric power dam at the location: latitude 6.261835° and longitude 0.003249°. At this specified location, the average wind speed and wind power density at 100m and 150m are 7.43 m/s, 381 W/m² and 8.02 m/s 477 W/m² respectively (GWA, 2023a). However, the wind potential is more concentrated during the night and very low during the daytime (GWA, 2023b, 2023a).

The study areas we have chosen are located in the Guinean climatic zone of West Africa, therefore the weather conditions are not severe. The ambient temperature is not very high. The maximum temperature is around 36.7°C and the minimum is around 19.75°C. The Figure 3.2-3 below shows that the first four months of the year are hotter. The temperature, gradually decreases from the fourth to the tenth month of the year and slightly increases afterward. This profile of the temperature is due to the behaviour of the climatic variability of the Guinean climatic zone. The period where the temperature decreases in the raining period

which causes the temperature to drop. The period with higher temperature corresponds to the dry season.

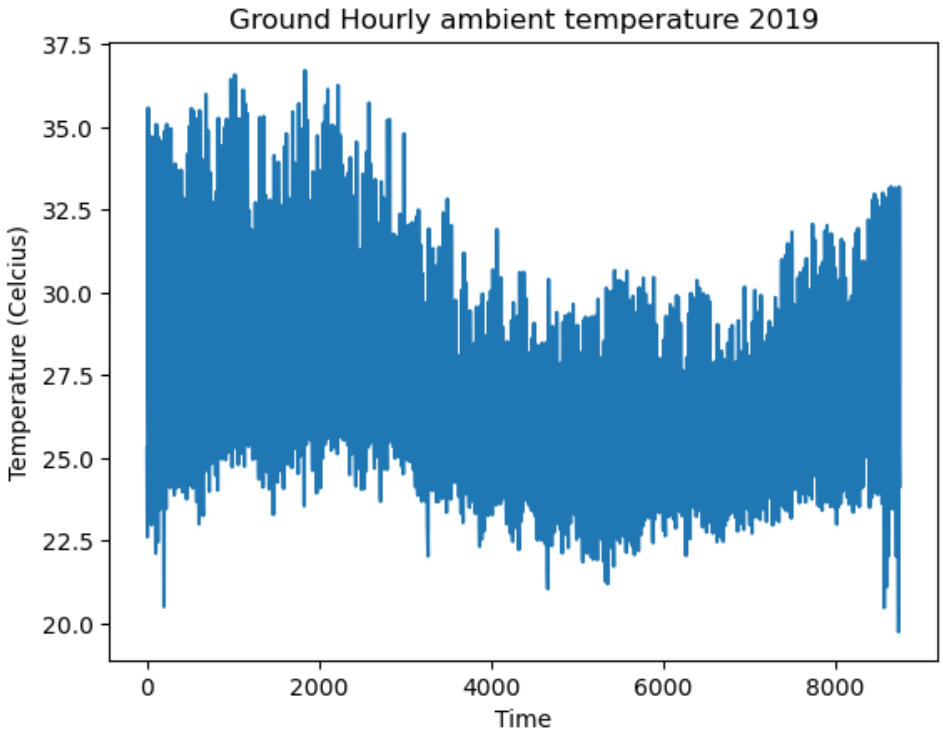

Figure 3.2-3: Hourly temperature of the year 2019

(Stefan & Iain, 2023)

Regarding the water resource, the discharged the downstream water of the dam will be used to feed the hydrogen production. Since the purpose of the dam is to generate electricity, feeding the hydrogen production plant with the upstream water can highly influence negatively the upstream water level therefore impact the dam electricity production. The daily variation of the downstream water level of the dam is shown in the Figure 3.2-5. The level of the downstream water is highly influenced by the quantity of water released or discharged (See Figure 3.2-4) during the operation of the dam. The lesser the quantity of water discharged, the lower the level of water is. Additionally, due the continual water flow of the water, the level varies rapidly. However, regarding the water level at the upstream of the dam, the variation is noticeable at seasonal scale (See Figure 3.2-6). Figure 3.2-6 shows that from the first six months (January to June) the level decreases linearly. This can be explained by the fact that this period corresponds to the dry season during which there is not rainfall to fill the dam. However, from the sixth month of the year, the water level starts increasing till the tenth month of the year (October) which corresponds to the raining season and decreases afterward; this marks the beginning of the dry season.

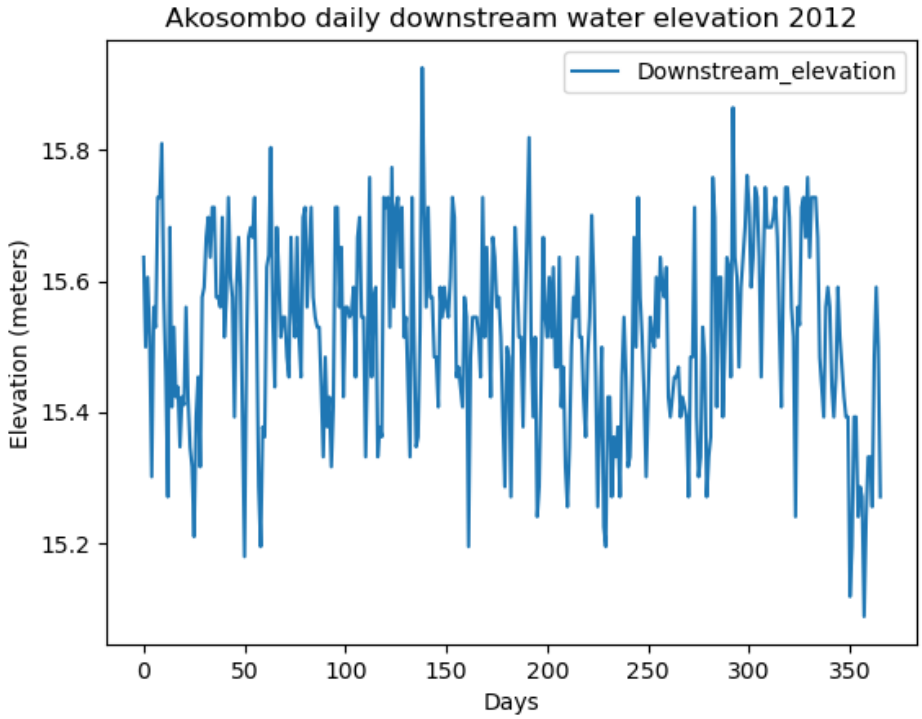

Figure 3.2-5: Akosombo dam daily downstream water elevation of the year 2012 (VOLTA RIVER AUTHORITY, 2006)

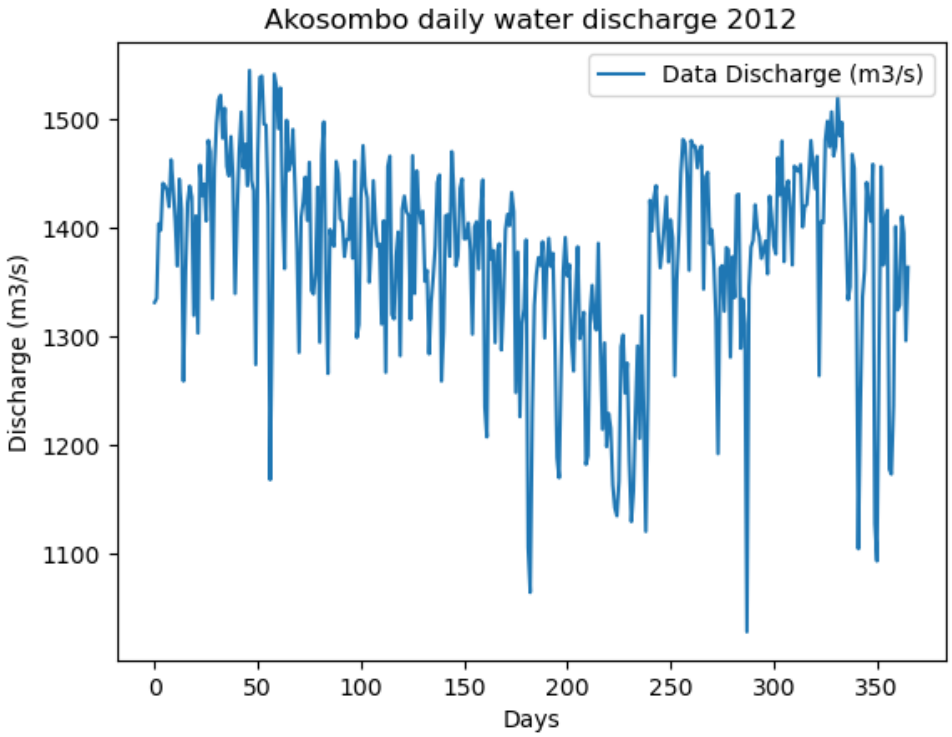

Figure 3.2-4: Akosombo daily water discharge of the year 2012 (VOLTA RIVER AUTHORITY, 2017)

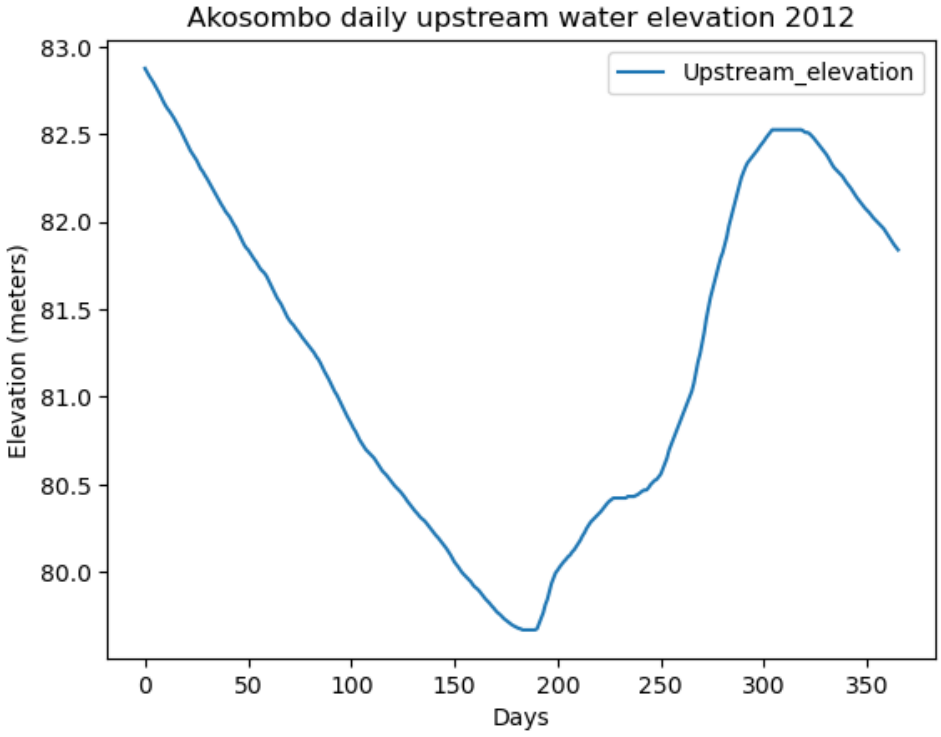

Figure 3.2-6: Akosombo dam daily upstream water elevation 2012 (VOLTA RIVER AUTHORITY, 2015)

3.3 Data and parameters

In this work, several renewable energy systems are considered such as land solar PV, floating solar PV, wind power and battery storage. Moreover, to produce green hydrogen, other necessary components such as an ultrapure water system, water pumping-piping and storage, electrolyzer, hydrogen compressor and storage. Therefore, the data required are more related to the operational variables of the system such as climate data (temperature, wind speed, solar radiation, water temperature, etc.) whereas the parameters as more linked to the design variables of the components such as economic parameters (capital expenditures (CapEx), operation expenditures (OpEx), nominal discount rates, the lifetime of the components, oxygen price etc) and components performance parameters (efficiencies, carbon emissions factors etc).

3.3.1 Data collection

The data used in this work are from the two study sites Bonkoko and Volta Lake in the year 2019, downloaded from climate data open sources and the parameters are taken from the

literature (articles, reports …). The weather data and demand data used in the model of this study have a time step of one hour. The ambient temperature data, the wind speed data, the global horizontal solar irradiation and air density data are downloaded from the Renewable Ninja climate data store (Pfenninger & Staffell, 2016). The water surface temperature is downloaded from the Copernicus Climate Change Service Climate Data Store (C3S-CDS, 2020). From those data, the power output factor of LPV, FPV, and wind turbines have been derived. For the demand data of hydrogen, we have elaborated an algorithm that generates the data depending on the profile of the power output of the plants.

3.3.2 Data processing

Data processing refers to the transformation of the raw data collected into a useful format to input into the model. In our work, the input data will be grouped into typical days representative of the days of the year 2019 called clustered data. To achieve this task, we make use of the Python tool to process the following data:

3.3.2.1 Lake surface water temperature retrieving and reshaping

The surface temperature of the water in Lake Volta is obtained from the Copernicus Climate Change Service climate database (C3S-CDS, 2020). The raw data covers all the lakes in the world from 1995 to the present day, at a daily resolution. It is, therefore, necessary to recover Lake Volta and reshape it at the hourly resolution, since this is the resolution used in this work. Figure 3.3-1 shows the procedure to get the hourly water surface temperature data.

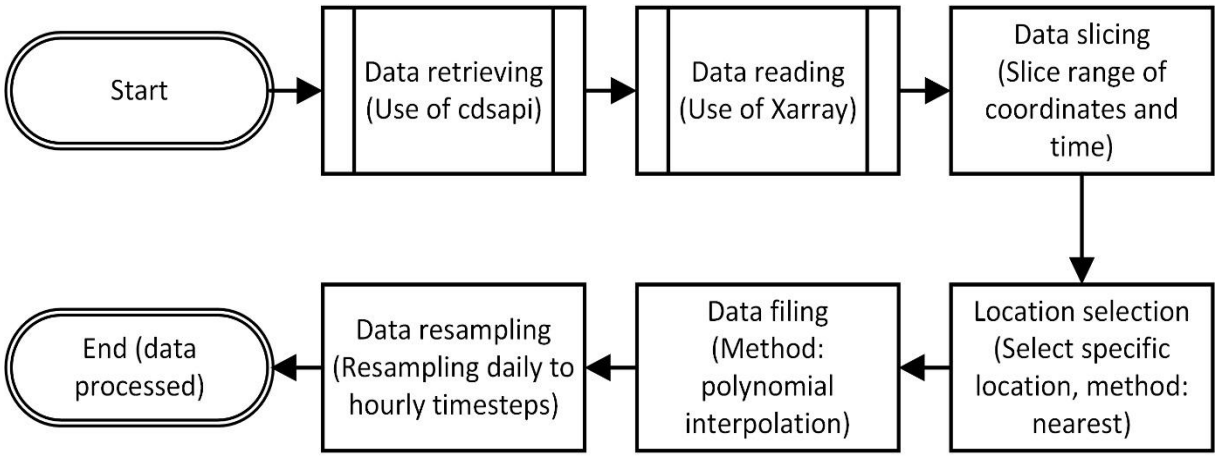

Figure 3.3-1: Algorithm chart flow of water surface temperature processing

The first step consists of downloading the global data of lake water surface temperature on the Copernicus Climate Change Service climate database and then reading it in the Python environment. The step forward consists of slicing the data to the considered lake

data using the coordinates and the time range, after that, we select a specific location in the lake to get the data using the “nearest” method. The missing values are filled using the polynomial interpolation method, afterwards, the data is resampled from daily to hourly timesteps.

3.3.2.2 Hydrogen demand data generation

As mentioned earlier, the goal of this model is to assess the economic technical aspect of a hydrogen production project. In our study, we consider a fixed amount of hydrogen that will be produced per day depending on the electricity output of the energy system. We generated hourly hydrogen production data for an entire year which depends on the solar PV and/or wind power output. Figure 3.3-2 shows the flowchart of the procedure. To do that, we created an algorithm based on weighted hours which steps are as follows:

- **Data input**: The input data, on an hourly basis, can be solar radiation or wind speed. In our case, we used electricity output expressed per unit of capacity, which depends on meteorological parameters. The data is read according to its format.
- **Data index setting**: The data time is set up as an index.
- **Index conversion**: The time indexed is converted to datetime with the desired datetime format which permits the functions used to identify the format of the data.
- **Data resampling to daily:** The hourly values of each day are summed up to form daily data.
- **Daily data resampling to hourly**: Hourly data is generated by upsampling the daily. In other words, on an hourly basis data is regenerated with each hourly having the daily value of its day.
- **Profile generation:** The weight of each hour is determined by dividing the initial input data by the daily data.

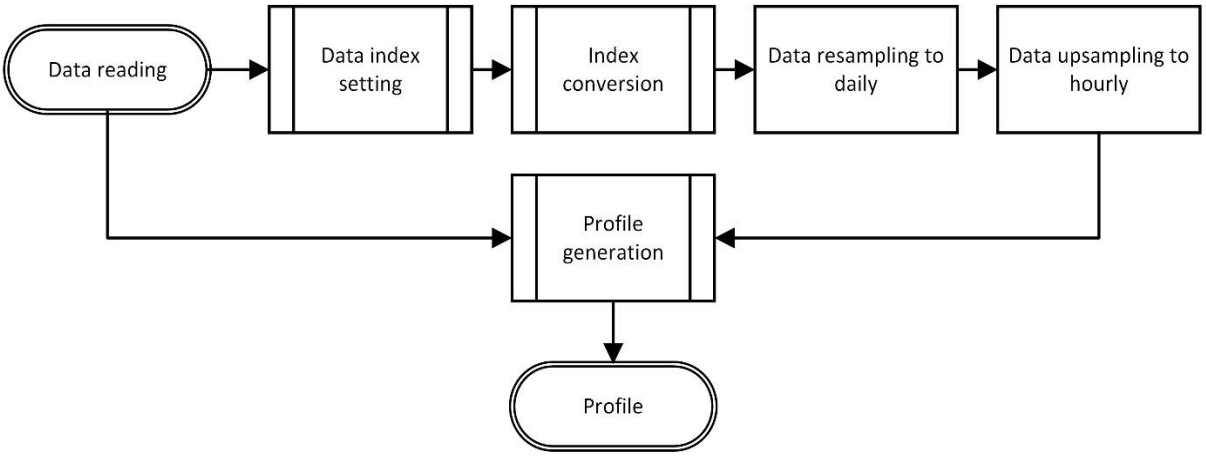

Figure 3.3-2: Algorithm chart flow of the power output profile generation

The hydrogen demand data is obtained by multiplying the total daily amount of hydrogen to be produced by this profile.

3.3.2.3 Data clustering

In most of the optimization problems that involve large sets of data, it is usual to encounter issues of handling large data with small timesteps. The most appropriate way is to cluster the data. Clustering data means identifying and grouping data within multidimensional data based on their similar patterns (Omran et al., 2007). There are several clustering methods some have been overviewed by (Omran et al., 2007). In general, the algorithm groups the data according to the number of clusters or representatives specified. The method used in this work is the K-medoids algorithm which is a classical partitioning technique of clustering that splits the data set of n objects into k clusters. It finds the most centrally located patterns in the clusters. Figure 3.3-3 shows the flow chart of the steps of the data clustering. The number of representative days or typical days is determined here by using the silhouette method. Silhouette method proceeds by analysing the average distances of each data point to its cluster and its nearest neighbouring cluster. Unlike most other methods, Silhouette is not only used to assess the validity of a complete cluster but can also be used to assess a single cluster or even a single data point to determine whether it is well grouped (Wang et al., 2017).

In this study, we cluster the solar PV output factor data of both locations, Bonkoko and Akosombo water reservoirs with 2 as the optimal number of clusters given by the silhouette method. The optimal number of clusters is given by the value that has the highest average silhouette score, here is 2.

The algorithm of the data clustering used in our work is as follows:

- **Input data**: The input data is the solar PV output
- **Hourly data conversion to daily**: Indexes of days and hours are set on the data which is unstacked. The obtained data is multi-indexed with the day index corresponding to the rows and the hours index corresponding to the columns.
- **Data normalizing:** To get the normalised values of the data, the data is divided by the maximum value of the data set
- **Clustering**: Depending on the optimal number of clusters entered, the K-medoids method is applied to fit the number of medoids found by iteration according to the data provided.

- **Scenario creation**: After the clustering, the indexes of the medoids found at compared with the indexes of the daily data to identify the daily data that are most representative. The identified days are the scenario days of typical days which represent the clusters.
- **Data weighting**: The sizes of the clusters are determined by grouping daily data according to their belonged cluster. These sizes are divided by the total size of all the clustered data.

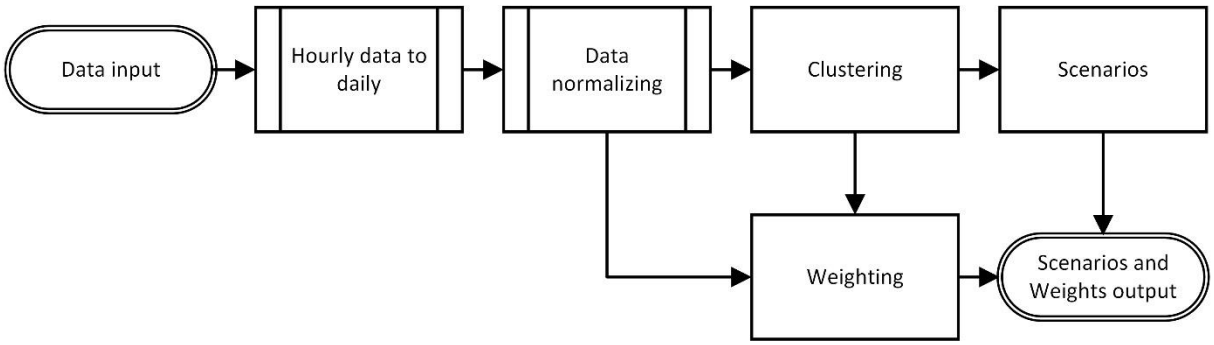

Figure 3.3-3: Algorithm chart flow of the PV output data clustering

3.4 Modelling

The renewable energy systems including the green hydrogen production plant are modelled within an energy system optimization framework. In our work, we used the COMANDO optimization framework.

3.4.1 Description of the energy system optimization framework COMANDO

The energy system optimization framework for components-oriented modelling and optimization for non-linear design and operation, COMANDO, is an open-source Python package (COMANDO Repository, 2021) designed to address the challenges of nonlinearities and dynamic effects raised by the required technical details of design and operation. The main goal of COMANDO is to offer an accessible ESMF in which energy systems components can be created in detail including differential-algebraic and nonlinear elements and aggregate them to system models for optimization. However, COMANDO is designed for small to medium energy systems e.g., district energy systems, industrial sites, or energy conversion processes. It is a flexible tool in the sense that doesn't include any specialized solution method but rather allows the user to intuitively build his components models, and system models, formulate his problem and define his desired solution approach (Langiu et al., 2021).

The modelling step is one of the most important parts meaning that a model that describes as much as possible the behaviour of the components and the energy system should be generated. To reach this achievement, pieces of information about the components and

their connectivity are required. For a generic component in COMANDO, the expected elements are design variables, operational variables, parameters, expressions, constraints, states, and connectors. Figure 3.4-1 shows the workflow for modelling, problem formulation, and optimization using COMANDO

The step of problem formulation consists of creating a problem with a design objective aggregating the costs of all the components, an operational objective that aggregates the inflow and outflow energy costs and other elements such as parameter values and additional constraints. As it is an optimization that is performed, the total costs of the energy system have to be as minimal as possible. Many optimizing solvers are used in energy system optimization, among which we can cite Gurobi, MAiNGO, BARON, etc. For our study, we will use the Gurobi optimizer package which can be used in several programming languages such as Python, C++, MATLAB, R, etc.

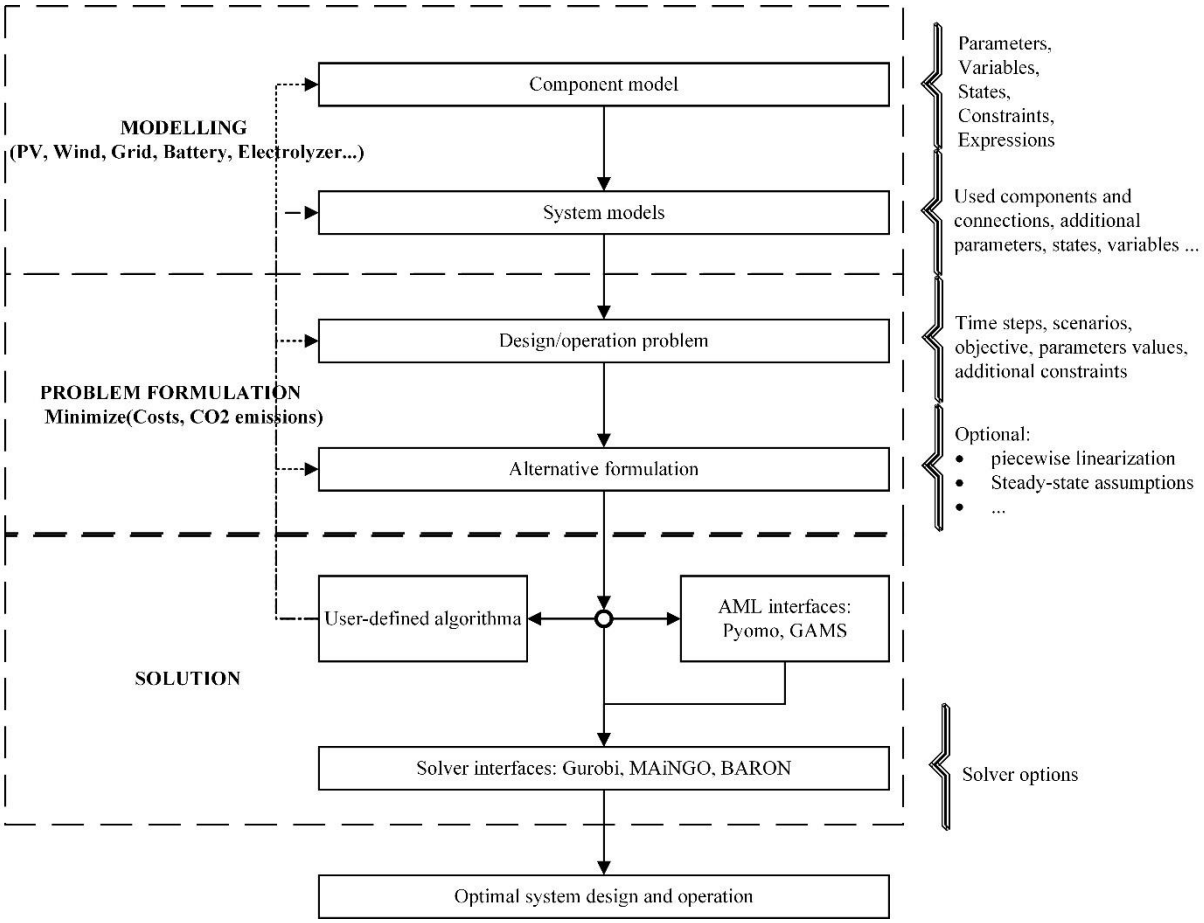

Figure 3.4-1: Workflow for modelling, problem formulation, and optimization using COMANDO. *Adapted from* (Langiu et al., 2021)

3.4.2 Description and modelling of the energy systems' components

3.4.2.1 Solar land PV

3.4.2.1.1 Land solar PV system description

Land PV systems also called ground-mounted PV systems are known to be large utility-scale solar power plants. The solar modules are held in place by racks or frames attached to ground mounting supports. Land PV mounting supports are composed of:

- Pole mounts which are driven directly into the ground or fixed in concrete,
- The foundation supports, such as concrete slabs or poured footings
- Ballasted footing mounts, such as steel or concrete bases use weight to fix the solar module system in position and do not need to penetrate the ground. (Sahu et al., 2016)

3.4.2.2 Land solar PV system modelling

The solar PV system constitutes the generator which provides electricity from solar radiation. It includes the PV modules and the inverter which converts the direct current into alternative current. For both land PV systems and floating PV systems, the electricity output is given by the following expression:

$$Elec_{output} = Size_{PV} * P_{factor} \quad 3.4\text{-}1$$

Where $Elec_{output}$ represents the electricity output in kWh, $Size_{PV}$ is the capacity of PV to be installed in kWp, P_{factor} is the PV power factor whether for the land or floating PV.

The PV power factor is dependent on climate factors such as irradiation, ambient temperature, wind speed and additionally lake surface water temperature for the floating PV.

The land PV and floating PV power factor is determined by using the following equation:

$$P_{factor} = \frac{P_{output}}{P_{STC}} \quad 3.4\text{-}2$$

With the different power given by the equation (Skoplaki & Palyvos, 2009):

$$P_{output} = A * \eta_{real} * I \quad 3.4\text{-}3$$

$$P_{STC} = A * \eta_{ref} * I_0 \quad 3.4\text{-}4$$

Where A is the area of the solar PV module. We will assume $A = 1\ m^2$, η_{real} is the instantaneous efficiency of the solar PV module that is a function of the environmental parameters.

The determination of the real efficiency requires the cell temperature that will be evaluated from the following equation which is a function of t cell temperature (Akhsassi et al., 2018;

Divya Mittal et al., 2017; Dubey et al., 2013; Mattei et al., 2006; Niyaz et al., 2021; Rahaman et al., 2023; Sachenko et al., 2020; Skoplaki & Palyvos, 2009):

$$\eta_{PV} = \eta_{ref}\left[1 + \beta_{ref}\left(T_{cell} - T_{ref}\right)\right]\left[1 + \gamma\, ln\left(\frac{I}{I_0}\right)\right] \quad 3.4\text{-}5$$

Where η_{PV} is the theoretical efficiency of the PV module, $\eta_{ref} = 19.9\%$ is the reference efficiency of the monocrystalline PV module at the standard test conditions (STC) (Ramasamy et al., 2021; Ramasamy & Margolis, 2021), ($T = 25℃$, $Irradiation = 1000W/m^2$, $AM1.5$) (King et al., 2004). $T_{ref} = 25℃$ is the reference temperature at the standard test conditions, T_{cell} is the cell temperature of the PV module. $\beta_{ref} = \frac{1}{T_0 - T_{ref}}$ is the temperature coefficient, $T_0 = 270℃$ is the highest temperature at which the efficiency drops to zero for crystalline silicon solar cells. $\beta_{ref} = 0.00408\ ℃^{-1}$, Dubey et al., 2013.. This coefficient means that each time the temperature rises to 1 ℃, the efficiency drops to 0.408%. $\gamma = 0.12$ is the solar radiation coefficient. I is the radiation received by the solar PV module in $\frac{W}{m^2}$. $I_0 = 1000\ \frac{W}{m^2}$ is the standard radiation

The cell temperature is expressed as a function of the module temperature and irradiation (King et al., 2004; Prilliman et al., 2020):

$$T_{cell} = T_m + \frac{I}{I_0}\Delta T_0 \quad 3.4\text{-}6$$

Where T_m is the back-surface module temperature, $\Delta T_0 = [2 - 3]℃$ is the temperature difference between the cell and the module back surface at an irradiance level of 1000 W/m^2

In our work, for land PV system, the module temperature is determined using the following equation (King et al., 2004):

$$T_m = T_a + Ie^{a+bV_w} \quad 3.4\text{-}7$$

Where T_a is the ambient temperature in degrees Celsius, V_w is the local wind speed in m/s, a is an empirically determined coefficient establishing the upper limit for module temperature at low wind speeds and high solar irradiance. b is an empirically determined coefficient establishing the rate at which module temperature drops as wind speed increases (a=-3.56 and b=-0.075 s/m)

After integrating all the equations, we found the final equation of the electricity output expressed as:

$$Elec_{output} = Size_{PV} * \frac{A * I * \eta_{ref}\left[1 + \beta_{ref}\left(T_m + \frac{I}{I_0}\Delta T_0 - T_{ref}\right)\right]\left[1 + \gamma\, ln\left(\frac{I}{I_0}\right)\right]}{A * \eta_{ref} * I_0} \quad 3.4\text{-}8$$

For the LPV system, the value of T_m is given by equation 3.4-7

3.4.2.3 Floating PV

3.4.2.4 Floating solar PV system description

A floating PV system is a PV generator that is typically installed over a water body such as water reservoirs, lakes, seas, etc. Since there is no solid support on the water body where to install the PV modules, a particular mechanism is developed to withstand the weight of the PV modules preventing them from diving. A floating PV plant is generally constituted of a flotation device with enough buoyancy to enable heavy loads to float called a pontoon. The pontoon is a combination of multiple floats made typically of high-density polyethene (HDPE). To secure the floating platform and prevent it from turning or floating away, an anchoring and mooring system is usually used to tie the platform to bollards or banks and lash at each corner. Additional components are the PV modules and the cables and connectors which should be enough robust to challenge high temperatures, long-term salt exposure and corrosion (Sahu et al., 2016).

Figure 3.4-2: Floating PV system on a water body in Netherlands

(EMILIANO, 2017)

3.4.2.5 Floating solar PV system modelling

The determination of the electricity output from the FPV uses the same equation 3.4-8 as for the LPV. However, the module temperature is different as it is a function of the ambient

temperature, the solar radiation, the wind speed and the water temperature (Charles et al., 2018).

$$T_m = 1.8081 + 0.9282T_a + 0.021I - 1.2210V_w + 0.0246T_w \quad 3.4\text{-}9$$

Where T_w represents the water temperature in degrees Celsius.

The final equation is obtained by integrating the above equation into equation 3.4-8

The economic parameters are summarized in Table 3.4-1. The total installed costs include the total equipment costs, total direct and indirect labour costs, total EPC other and overhead costs and total development costs (Ramasamy et al., 2021) meaning that land acquisition and inspection costs for land PV and the site staging costs of the water body are included (Ramasamy & Margolis, 2021).

Table 3.4-1: Economic parameters of the solar PV systems

Parameters	**Land PV**	**Floating PV**	**Sources**
CapEx [€/kW]	798.07*[1]	920.85*[2]	(Ramasamy et al., 2021)[1], (Ramasamy & Margolis, 2021)[2]
OpEx [€/kW/year]	15.8*	13.6*	(Ramasamy & Margolis, 2021)
Efficiency [%]	19.9	19.9	
Lifetime [years]	30	30	(Ramasamy & Margolis, 2021)
Replacement costs [€/kWh]	0	0	---------
CO_2 factor [g CO2eq/kWh]	50	50	(NREL, 2012; Terlouw et al., 2022)

*Note: values with * are converted from 2020USD-based to 2020Euro-based(0.877Euro/USD)*

The nominal discount rate is assumed 0.074 (Steffen, 2020) for all the components

3.4.2.6 Wind turbine modelling

The wind turbine is a renewable energy technology that provides electricity thanks to wind speed. The working principle is the conversion of the kinetic energy of the wind into mechanical energy and then into electrical energy through a generator. The electricity output of a wind turbine is calculated with the following equation:

$$Elec_{output} = Size_{wind} * P_{wind_{factor}} \quad 3.4\text{-}10$$

Where $Elec_{output}$ in kWh, $Size_{PV}$ is the capacity of wind turbines to be installed in kilowatt-peak, P_{factor} is the wind turbine power factor in kWh/kWp

The wind power factor is a key parameter to determine the wind electricity output. This parameter is expressed as:

$$P_{wind_{factor}} = \frac{P_{wind_{output}}}{P_{max}} \quad \text{3.4-11}$$

The wind power output is expressed as in the following equation (Martinus & Venter, 2017):

$$P_{wind_{output}} = \begin{cases} 0 & if\ V < V_{cut_{in}} \\ \frac{1}{2}\rho A V^3 C_p & if\ V_{cut_{in}} < V < V_{cut_{out}} \\ 0 & if\ V > V_{cut_{out}} \end{cases} \quad \text{3.4-12}$$

Where $P_{wind_{output}}$ is the power output in W, ρ is the density of the air in kg/m^3, A is the swept area in m^2, V is the wind speed in m/s, $V_{cut_{in}}$ is the cut in wind speed 3 m/s and $V_{cut_{out}}$ is the cut-off wind speed of 22 m/s for the model: V100-2.0 MW® IEC IIB (Vestas, 2023), C_p is the efficiency coefficient of the wind turbine, Cap_{fact} is the capacity factor of the wind turbine expressed as the annual real electricity output over the annual maximum electricity output and P_{max} being the maximum power that the wind turbine can deliver in the optimum conditions. In our study, we will do our assumptions and calculations based on the characteristics of a 2MW wind turbine (model: V100-2.0 MW® IEC IIB) (Vestas, 2023). The characteristics taken into consideration in our calculations are listed in Appendix *4*.

We do our assumptions as follows:

A =7,854 m^2

$\rho = 1.218 \frac{\text{kg}}{\text{m3}}$ Assumption based on (Williams, 1949)

C_p = 0.11 to 0.5 efficiency coefficient of 2 MW wind turbine (model: E82E2) from 2-18 m/s wind speed (Josué, 2013). In our work, we will assume 0.45 as the average efficiency coefficient for 3 to 12 m/s wind speed with 9 m/s as optimal wind speed.

P_{max} is calculated with equation 3.4-12. The considerations done: $\rho_{std} = 1.218 \frac{\text{kg}}{\text{m3}}$, $V_{opt} = 13 \frac{m}{s}$, $C_{p_{\max}} = 0.593$ (Josué, 2013), A =7,854 m^2

$$P_{max} = \frac{1}{2}\rho_{std} A V_{opt}^3 C_{p_{max}} \quad \text{3.4-13}$$

The final expression used for the wind power factor generation is as follows:

$$P_{wind_{factor}} = \frac{\rho A V^3 C_p}{2P_{max}} \quad 3.4\text{-}14$$

The final expression of the electricity output from the wind turbine is given by:

$$Elec_{output} = Size_{wind} * \frac{\rho V^3 C_p}{\rho_{std} V_{opt}^3 C_{p_{max}}} \quad 3.4\text{-}15$$

Table 3.4-2 summarises the economic parameters used in the modelling.

Table 3.4-2: Economic parameters of the wind turbines

Parameters	Wind turbines	Sources
CapEx [€/kW]	1282.2*	(Stehly & Duffy, 2020)
OpEx [€/kW/year]	37.71*	
Efficiency factor [%]	45	Assumed from (Josué, 2013)
Lifetime [years]	25	(Stehly & Duffy, 2020)
Replacement costs [€/kWh]	0	---------
CO_2 factor [g CO2eq/kWh]	52.7	(Bhandari et al., 2020)

*Note: values with * are converted from 2020USD-based to 2020Euro-based(0.877Euro/USD)*

3.4.2.7 Batterie storage modelling

Battery storage is a key component of renewable energy systems. It accumulates the electricity and delivers it when there is not enough or no electricity production from the renewable plant. In the ESOF COMANDO, the battery storage is modelled based on a cyclic mode of operation expressed as follows:

$$\begin{cases} \varphi_{ch} = \xi_{in} - \xi_{out} - \sigma_{dis} \\ \phi_{ch} = f(\varphi_{ch}, \iota_{st}) \end{cases} \quad 3.4\text{-}16$$

Where ξ_{in} and ξ_{out} are respectively the amount of electricity getting in and getting out, φ_{ch} is the rate of change, ϕ_{ch} is the state of change of the electricity storage, ι_{st} is the initial state, σ_{dis} is the losses due to self-discharge

Table 3.4-3 shows the parameters included in the battery storage modelling.

Table 3.4-3: Economic parameters of battery storage

Parameters	Battery storage	Sources
CapEx [€/kWh]	1099.54*	(NREL, 2022)
OpEx [€/kWh/year]	2.5% of CapEx	

Efficiency [%]	98	Assumed
Lifetime [years]	15	(ABB, 2021)
Replacement costs [€/kWh]	739*	Assumed from (NREL, 2022)
CO_2 factor [g CO2eq/kWh]	216	(Romare & Dahllöf, 2017)

*Note: values with * are converted from 2021USD-based to 2021Euro-based (0.8458Euro/USD)*

The CapEx of the battery storage is assumed $1300/kWh taking only into the consideration Battery central inverter, Electrical BOS (Balance of the plant), Installation labour and equipment, Lithium-ion Bat cabinet, sale tax and Structural BOS. Moreover, the replacement cost of the battery (NREL, 2022).

3.4.2.8 Hydrogen storage modelling

Hydrogen storage is an important part of the hydrogen production plant in the sense that it serves to store the hydrogen produced during the operation time and supply the hydrogen needs. Its modelling is similar to battery storage. The main expressions are expressed as follows:

$$\begin{cases} \varphi_{ch} = H_{in} - H_{out} - \sigma_l \\ \phi_{ch} = f(\varphi_{ch}, \iota_{st}) \end{cases} \quad \text{3.4-17}$$

Where H_{in} and H_{out} are respectively the amount of hydrogen getting in and getting out, φ_{ch} is the rate of change, ϕ_{ch} is the state of change of the hydrogen storage, ι_{st} is the initial state, σ_l is the loss due to leakage.

Table 3.4-4: Economic parameters of hydrogen storage

Parameters	Hydrogen storage	Sources
CapEx [€/kgH_2]	306.95*	(Elberry et al., 2021)
OpEx [€/kgH_2/year]	1% of CapEx	(Gorre et al., 2020b)
Efficiency [%]	0.0057 kg/h losses	(Elberry et al., 2021)
Lifetime [years]	20	(Gorre et al., 2020b)
CO_2 factor [g CO2eq/kgH_2]	5	Assumed

*Note: values with * are converted from 2020USD-based to 2020Euro-based(0.877Euro/USD)*

3.4.2.9 Electrolysers

3.4.2.10 Electrolysers' description

Electrolyzers can be classified according to the electrolyte used, which separates the electrolyzer into two compartments. The first one is called the anode where an oxygen conversion reaction occurs and another one is the cathode where a hydrogen conversion reaction occurs. The main technologies are alkaline electrolyzer (AEL), proton exchange membrane electrolyzer (PEME) and solid oxide electrolyzer (SOEL). The principles, reactions and properties of AEL, PEMEL and SOEL are described below.

3.4.2.10.1.1 Alkaline electrolyzer

Alkaline electrolyzer, nowadays is the most mature technology already used in large-scale hydrogen production. The electrodes are plunged into an alkaline electrolyte, usually a 25–30% aqueous KOH solution, compartmented by a membrane. The electrolyte is stored in two separate containers for each gas produced (O_2 and H_2), which also act as a gas-liquid separator. The produced gas has high quality after drying and is typically ranged from 99.5–99.9% for H2 and 99–99.8% for O_2 (Buttler & Spliethoff, 2018). The operation temperature of the AEL is ranged from 70-90℃ and the output pressure is below 30 bar (Shiva Kumar & Lim, 2022). The partial reaction at the electrodes is given by:

$$2H_2O + 2e^- \longrightarrow H_2 + 2HO^- \quad Cathode \qquad 3.4\text{-}18$$

$$2HO^- \longrightarrow \frac{1}{2}O_2 + H_2O + 2e^- \quad Anode \qquad 3.4\text{-}19$$

For this technology of electrolyser, the energy required to produce an Nm^3 of hydrogen is 4.4 kWh (ISPT, 2020) meaning around 54.54 kWh per kilogram of hydrogen. Considering the lower heating value of hydrogen 33.33 kWh/kgH_2 (Bhandari, 2022), one can deduce an efficiency of electrolysis around 61.112%.

3.4.2.10.1.2 Proton exchange membrane electrolyzer

The membrane used for this type of electrolyser is a proton exchange membrane, in most cases Nafion membrane, that separates the two half-cells. The electrodes are usually directly fixed on the membrane forming the membrane electrode assembly (MEA). Water is input at the anode and partly transported to the cathode side due to the electroosmotic effect. Due to its very low cross-permeation, the proton exchange membrane provides higher purity of hydrogen than AEL, typically greater than 99.99% after drying (Buttler & Spliethoff, 2018) The operation temperature of the PEME is ranged from 50-80℃ and output pressure is below 70 bar (Shiva Kumar & Lim, 2022). The following partial reactions take place:

$$2H^+ + 2e^- \longrightarrow H_2 \ \ Cathode \qquad 3.4\text{-}20$$

$$H_2O \longrightarrow \frac{1}{2}O_2 + 2H^+ + 2e^- \qquad 3.4\text{-}21$$

For the technology of PEME, the energy requirement is around 4.9 kWh for an Nm^3 of hydrogen (ISPT, 2020) corresponding to 48.972 kWh to produce a kilogramme of hydrogen. Based on the same low heating value considered for the alkaline, the efficiency is around 68.06%.

3.4.2.10.1.3 Solid oxide electrolysis cells

Solid oxide electrolyzer operates at very high temperatures ranging between 700–900 °C and the output pressure of the hydrogen is around 1 bar (Shiva Kumar & Lim, 2022). Due to its high-temperature operation, the efficiency is higher than AEL and PEME. However, SOEL has remarkable challenges regarding material stability. The advantages in terms of efficiency result from improved kinetics, thermodynamics that favour the use of internal heat at higher temperatures and the conversion of water vapour. The SOEL offers interesting features such as the ability to co-electrolyse CO_2 and steam-producing syngas containing H_2 and CO for fuel synthesis and the ability to work irreversibly as a fuel cell. However, SOEL remains at the research stage for single-cell or short-stack tests (Buttler & Spliethoff, 2018). The reactions at the electrodes are:

$$H_2O + 2e^- \longrightarrow H_2 + O^{2-} \ \ Cathode \qquad 3.4\text{-}22$$

$$O^{2-} \longrightarrow \frac{1}{2}O_2 + 2e^- \ \ Anode \qquad 3.4\text{-}23$$

The technology of SOEC requires less energy than the other technologies which allows it to achieve an efficiency of 83% (Barwe et al., 2023).

3.4.2.10.2 Electrolyzer modelling

The electrolyser is the central component of a hydrogen production plant. It uses the energy heat and/ or electricity to split the water into oxygen and hydrogen. Depending on the technology of the electrolyser used, the efficiency differs and the amount of water required differs too. The electrolyser model is based on the water and electricity required to produce a certain amount of hydrogen and oxygen. The below table summarises the economic parameters of the electrolyzers used in our model.

Table 3.4-5: Summary of economic parameters of AEL, PEME and SOEC

Parameters	AEL	PEME	SOEC	Sources
CapEx [€/kW]	1400[1]	1800[1]	2800[2]	(ISPT, 2020)[1], (Francesco Pavan et al., 2023)[2]
OpEx [€/kW/year]	2 % of CapEx	2 % of CapEx	2 % of CapEx	Assumed
Efficiency [%]	68.1[1]	61.12[1]	83[2]	Calculation based on (ISPT, 2020)[1], (Barwe et al., 2023)[2]
Lifetime [Hours]	100000[1]	90000[1]	93000[2]	(Escamilla et al., 2022)[1] (Harboe et al., 2020)[2]
Replacement costs [€/kW]	104[1]	270[1]	1220[2]	Calculation based on (ISPT, 2020)[1], (Barwe et al., 2023)[2]
CO2 factor [g CO2eq/kgH_2]	86 to 138 assumed 100			(Vincent Knop, 2022)

For the model to behave as much as possible as its working principle describes, it is important to set some constraints on the design and operational variables.

Constraints

$$\begin{cases} \xi_{in} = \left(\frac{k_{H2} * LHV_{H2}}{\eta_{elec}}\right) * \psi_{H2O_{in}} \\ H_{out} = \left(\frac{\eta_{elec}}{LHV_{H2}}\right) * \xi_{in} \\ O_{out} = k_{O2} * \psi_{H2O_{in}} \end{cases} \quad 3.4\text{-}24$$

Where ξ_{in} is the electricity getting in the electrolyzer in kWh, $Hydrogen_{output}$ is the hydrogen getting out of the electrolyser in kgH_2, $\psi_{H2O_{in}}$ is the ultrapure water getting in the electrolyser in kilograms, O_{out} is the oxygen obtained from the electrolysis in kilogram. η_{elec} is the efficiency of the electrolyser, LHV_{H2} is the hydrogen low heating value being 33.33 kWh/kgH_2 (Bhandari, 2022), $k_{O2} = 0.888$ and $k_{H2} = 0.112$ are respectively the mass percentage of oxygen and hydrogen in 1 kilogram of water.

3.4.2.11 Hydrogen compressor modelling

The hydrogen compressor is essential for the hydrogen production plant to compress hydrogen for storage, transporting with trucks, hydrogen refuelling stations, etc. The compression work required a certain amount of electricity to power the compressor. The power required is expressed as follows (Gökçek & Kale, 2018):

$$Power_{required} = C_p \frac{T_1}{\eta_c}\left[\left(\frac{P_2}{P_1}\right)^{\frac{r-1}{r}} - 1\right]\dot{m}_c \quad 3.4\text{-}25$$

Where, C_p is the specific heat of hydrogen at constant pressure ($14.304\,\text{kJ/kg K}$ or $0.003973\,\text{kWh/kg K}$ /), T_1 is the inlet gas temperature of the hydrogen (293 K), η_c is the compressor efficiency (0.75), $P_1\ and\ P_2$ represent respectively the inlet and output gas pressures of the hydrogen compressor (P_1 =14 bar, P_2=160 bar), r is the isentropic exponent of hydrogen (r = 1.4), $\dot{m}_c$ is the gas flow rate through the hydrogen compressor in kilograms per second (kg/s) but for our case

Constraints

$$\begin{cases} H_{in} \leq \chi_{comp} \\ \xi_{in} = P_{req} \\ H_{out} = H_{in}\,, assuming\ no\ losses \end{cases} \quad 3.4\text{-}26$$

Where χ_{comp} is the size of the hydrogen compressor, H_{in} and H_{out} are the hydrogen input and output respectively. ξ_{in} in the electricity input and P_{req} is the power required to compress the hydrogen.

Table *3.4-6* shows the economic parameters of the hydrogen compressor.

Table 3.4-6: Economic parameters of hydrogen compressor

Parameters	Hydrogen Compressor	Sources
CapEx [€/kW]	2440	(Terlouw et al., 2022)
OpEx [€/kW/year]	4% of CapEx	
Efficiency [%]	No losses	Assumed
Lifetime [years]	20	Assumed
Replacement costs [€/kW]	Assumed no replacement	Assumed
CO_2 factor [g CO2eq/kgH_2]	5	Assumed

3.4.2.12 Ultrapure water system modelling

The operation of the electrolysers requires a certain purity of the water to achieve efficient and longer operation and lifetime. Ultrapure water treatment system is therefore essential to be combined with the hydrogen production plant. According to (Becker et al., 2023), contamination and impurity accumulation poison the electrolysers and can highly impact their performance of the electrolysers. Therefore, impurities such as Ca^{2+}, Mg^{2+}, and

Cl^- need to be removed. Some of the water purification technologies are reverse osmosis and ion exchange resin technologies which permit to achieve the ISO 3696 Grade 2 water requirements, which have a conductivity of <1.0 mS cm^{-1} (Tsotridis & Pilenga, 2021).

The modelling of the ultrapure water purification system is based on the untreated water and electricity required to obtain 1 cubic meter of ultrapure water. Typically, the production of 1 kilogram of green hydrogen requires 9 kilograms of ultrapure water which can be obtained by purifying groundwater, surface water, wasted water or seawater through water desalination. Depending on the source of the raw water, the energy and untreated water requirements differ. To get 1 cubic meter of ultrapure water 1.4 m^3 and 2.8 kWh are required for groundwater, 1.5m^3 and 3.3kWh for surface water and 3.3 m^3 and 23.1 kWh for seawater (Tsotridis & Pilenga, 2021). In our work, we will be using the downstream water of the Akosombo dam to produce green hydrogen. We considered, therefore, the requirements for surface water to model our ultrapure water purification system.

Constraints

$$\begin{cases} \psi_{H2O_{out}} \leq \chi_{H2O_{pur}} \\ \xi_{in} = \omega_{in} * r_1 \\ \psi_{H2O_{out}} = \xi_{in} * r_2 \end{cases} \quad \text{3.4-27}$$

Where ω_{in} is the raw water input in litres, $\psi_{H2O_{out}}$ is the ultrapure water output in litres, $\chi_{H2O_{pur}}$ is the size of the water purifier in litres/hours. It translates the capacity of producing ultrapure water per hour, r_1 is the electricity-raw water ratio for surface water in kWh/litre of surface water (3.3/1500 kWh/l). r_2 is the ultrapure water-electricity ratio for surface water in litres of ultrapure water per kWh of electricity (1000/3.3 l/kWh). ξ_{in} is the electricity getting in the ultrapure water system.

The economic parameters of the ultrapure water system are summarized in the following Table *3.4-7*:

Table 3.4-7: Economic parameters of the ultrapure water system

Parameters	Ultrapure water system	Sources
CapEx [€/m^3/h]	2376.4*	(Quotation - 2000LPH Ultrapure Water Treatment Plant, 2023)
OpEx [€/m^3/h /year]	249* for 12/24h of operation	(Consumable Table - 2000LPH Ultrapure Water Treatment Plant, 2023)
Lifetime [years]	15	Assumed

Replacement costs [€/m³/h]	2376.4*	(Quotation - 2000LPH Ultrapure Water Treatment Plant, 2023)

*Note: values with * are converted from 2023USD-based to 2023Euro-based*

3.4.2.13 Water pumping-piping and storage modelling

For both land-based and floating-based energy systems, the water access point is the downstream water of the Akosombo Dam. Therefore, a water pumping-piping component is essential, particularly for the land PV system which is quite far from the Akosombo hydropower reservoir as well as the water storage to feed in water the hydrogen production plant. Since it is surface water, we will consider a surface water pump and horizontal pumping. To model this set of components we consider the electricity required for the pumping and piping. (Caldera et al., 2018) report that for horizontal pumping-piping, the electricity required is about 0.04kWh/(m³/h)/100 km.

Constraints of pumping-piping component

$$\begin{cases} \omega_{pp} \leq \chi_{pp} \\ \omega_{pp} = r * (\eta_w) * \xi_{in} \end{cases} \quad 3.4\text{-}28$$

Where ω_{pp} is the water pumped in cubic meters, χ_{pp} is the size of the system pump pipe in litres/hour, r is a ratio representing the amount of water pumped and piped per kWh of electricity. $\eta_w = 1 - l_{water}$ is the efficiency of the water pumping piping and l_{water} percentage of losses during water transport, ξ_{in} is the electricity input for the water pumping and piping in kWh.

The economic parameters of the pumping-piping and water storage systems are listed in the table below:

Table 3.4-8: Economic parameters of pumping piping and water storage system

Parameters	Pumping	Piping	Water storage	Source
CapEx [€]	200[€/m³/h/km][1]	3200 [€/km][2]	65 [€/m³][3]	(Caldera et al., 2018)[3], (Clark et al., 2002)[2], own assumption based on market price [1]
OpEx [€ /year]	2% of CapEx	16900 € [2]	2% of CapEx	
Lifetime [years]	30	30	30	
Replacement costs	0	0	0	----

3.4.2.14 Hydrogen demand modelling

The hydrogen production is in correlation with the production capacity of the hydrogen production plant. The purposes of hydrogen production are diverse such as oil refining, steel production, green ammonia production for fertilizer, etc. At the regional level, West Africa has several industry branches that use hydrogen in their processing. Among these industries, we can mention the oil refineries of Lagos, Port Harcourt, Kaduna and Warri in Nigeria, the Tema oil refinery in Ghana, etc. In addition, there are some green ammonia production plants planned and announced in Nigeria and Sierra Leone. Moreover, there is steel production located in Ghana, Liberia, and Nigeria which could require hydrogen in the process. At the global level, hydrogen production could be directly exported within Africa and worldwide via shipping.

For our study, we assume a daily production of 15 tons of green hydrogen. The hydrogen production data profile follows the variability of the renewable energy potential, meaning that the production is maximised during periods of high electricity production from renewable energy systems.

3.4.2.15 Oxygen selling option modelling

Oxygen is a by-product that constitutes around 88.8% of the water used for the electrolysis and represents 8 times the mass of hydrogen produced. Due to its high purity, oxygen from electrolysis can be introduced in a circular economy. For instance, electrolysis oxygen can be used in the operation of hydrogen fuel cells which require a certain purity of hydrogen, it can also be used in treatments in healthcare centres and hospitals, etc. Oxygen has a sales opportunity that can be exploited to amortize the cost of green hydrogen. Based on the study done by (Squadrito et al., 2018) to assess the feasibility of oxygen production from electrolysis for medical use, we estimate an ex-factory cost of 3$/kg$O_2$ (2.631€/kgO_2 with 2020USD to 2020Euro exchange rate).

3.4.2.16 Electricity injection into the grid option

The electricity produced from the renewable energy systems could at the pick production period exceed the electricity required by all the components which consume electricity. In this case, we assume a unidirectional connection to the grid only to inject the excess electricity.

3.4.3 Energy systems configurations

3.4.3.1 Land-based energy systems

The land-based energy systems are installed over the land. In our work, it will be installed at Bonkoko. We considered two configurations, one with only solar PV and a hybrid PV-Wind powering the hydrogen plant. Figure 3.4-3 represents the two configurations:

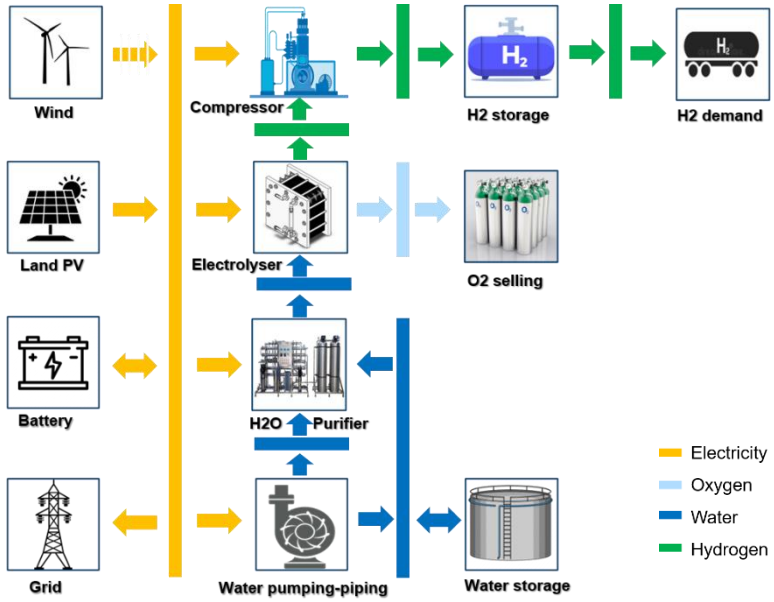

Figure 3.4-3: Land PV, hybrid Land PV-Wind energy systems configurations

3.4.3.2 Floating-based energy systems

The two configurations considered in this case are a floating PV installed over the Akosombo Dam water reservoir and a hybrid floating PV-Wind. However, in the second configuration, the wind turbines will be considered installed on land close to the water reservoir, next to the hydropower dam as well as the hydrogen production plant. The figure below shows the configurations of the floating PV energy system.

The dashed arrow of the wind in Figure 3.4-3 and Figure 3.4-4 means that there is a first configuration without the wind and a second including the wind.

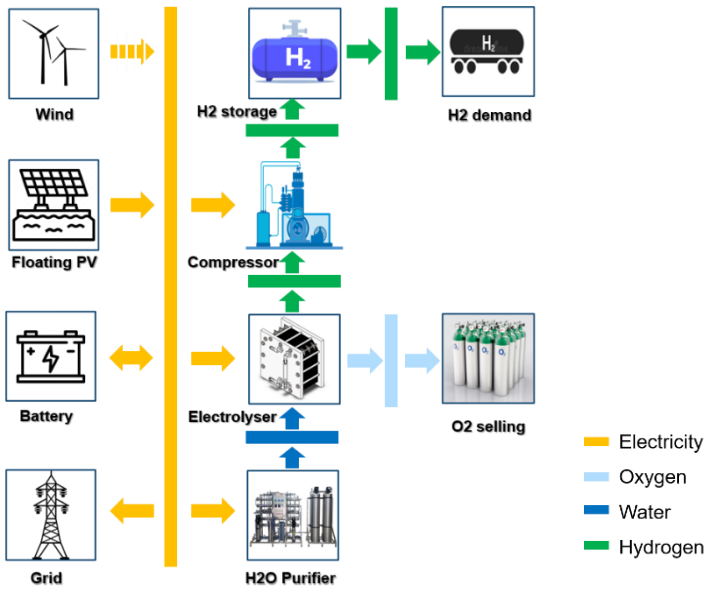

Figure 3.4-4: Floating PV, hybrid Floating PV-Wind energy systems configurations

3.4.4 Optimization problem

The optimization problem formulation is composed of two main objective functions: the design objective function and the operational objective function expressed as follows:

$$Op_{obj} = \sum_{i} Var_{costs}^{i} \quad 3.4\text{-}29$$

$$Des_{obj} = \sum_{i} Inv_{costs}^{i} + F_{costs}^{i}$$

Where:

$$Inv_{costs}^{i} = \sum_{i=component} (CapEx + R_{costs_i}) * \frac{d(1+d)^{n_i}}{(1+d)^{n_i}} \quad 3.4\text{-}30$$

$$F_{costs}^{i} = \sum_{i=component} OpEx_i \quad 3.4\text{-}31$$

Where Op_{obj} and Des_{obj} are respectively the operational objective function and the design objective function. $CapEx_i$ are the total capital expenditures and R_{costs_i} are the replacement costs of a considered component, Inv_{costs}^{i} represents the total annualized capital expenditures of all the components. d is the nominal discount rate (0.74%), n_i is the lifetime of a considered component. $OpEx_i$ is the annual operation and maintenance expenditures of a considered component. Var_{costs}^{i} are the costs implied by external sources or services involved in the operation of the plant (e.g., Buying electricity from the grid)

The cost optimization of an energy system implies minimizing the costs as much as possible while keeping the capability to provide the energy required all the moment. With the Gurobi optimizer, the direction of optimization of our energy systems cost minimization is expressed as:

$$Obj = min\big(\ Des\_obj\ , Op_{obj}\big) \qquad 3.4\text{-}32$$

3.4.5 Techno-economic assessment

A techno-economic model is an integrated process and cost model. It combines elements such as the modelling of the process itself, the sizing of the components, the total capital costs, and operating costs estimation. The optimization of the energy systems with the ESOF COMANDO gives the optimal sizes of the components and the optimal total costs. With the optimal costs, we can determine the levelized cost of electricity (LCOE) and levelized cost of hydrogen (LCOH) which are the key metrics to determine a project's feasibility.

3.4.5.1 Levelized costs of electricity

The calculation of the levelized cost of electricity is done by dividing the total lifetime costs of the project by the total amount of energy expected to be produced within its lifetime. It represents the average revenue per unit of energy generated that would be required to recover the total costs of a plant during an assumed financial life (EIA, 2022). The calculation of the LCOE is done with the following expressions (Gökçek & Kale, 2018):

$$LCOE = \frac{TAC_{PV/Wind_{Syst}}}{TEG_{an}} \qquad 3.4\text{-}33$$

$LCOE$ is the levelized cost of electricity in Euro per MWh, $TAC_{PV/Wind_{Syst}}$ are the total annualized costs of the solar PV plant or the hybrid solar PV-Wind in Euro, TEG_{an} is the total annual electricity generated in MWh.

3.4.5.2 Levelized cost of hydrogen

The LCOH is calculated with the following expression:

$$LCOH = \frac{TAC_{H2_{Syst}} + Elec_{H2_{prod}} * LCOE}{THG_{an}} \qquad 3.4\text{-}34$$

$TAC_{H2_{Syst}}$ are the total annualized costs of the components involved in the hydrogen production excluding solar PV and wind turbines [Euro], $Elec_{H2_{prod}}$ is the total electricity used for hydrogen production in Euro/MWh, THG_{an} is the total annual hydrogen generated in kilograms.

3.4.6 Water cooling impact on the cell temperature and efficiency

One of the advantages of the FPV is the water-cooling effect which lowers the close environment temperature of the PV module allowing them to operate at a lower cell temperature, unlike the LPV. To assess how impactful is the water-cooling effect on the PV, we will consider a PV plant installed over the Akosombo dam water reservoir and determine the cell temperature and the efficiency. We will consider the same PV plant installed over land with the same climatic conditions and calculate the cell temperature and efficiency. We will compare the two results and discuss them.

3.4.7 Water savings from FPV

FPV can reduce water evaporation, preserving a significant amount of water that can be essential for water bodies in regions where water is scarce. It is therefore necessary to assess the water evaporation rate which will allow us to estimate the amount of water saved from evaporation. To determine the evaporation rate, we will use the following expression (The Engineering ToolBox, 2004) modelled to estimate the evaporation rate of a lake:

$$g_h = \theta A(x_s - x) \qquad 3.4\text{-}35$$

Where g_h is the amount of evaporated water per hour (kg/h), $\theta = (25 + 19\,\mathrm{v})$ is the evaporation coefficient (kg/m^{2}h), and v is the velocity of air above the water surface (m/s). A is water surface area (m^2). This will correspond to the total area occupied by the FPV determined by the equation $A = \frac{FPV_{size}}{\eta_{ref} * I_0}$ derived from 3.4-4, x_s is maximum humidity ratio of saturated air at the same temperature as the water surface (kg/kg) (kg H_2O in kg dry air) and x is humidity ratio air (kg/kg) (kg H_2O in kg dry air).

3.4.8 Impact of water point proximity on the LCOH

The assessment of the water point proximity to the hydrogen production plant is to determine how much the water transport and storage impact the LCOH. To achieve this assessment, we will consider the LPV plant first installed at Bonkoko and determine the LCOH. Then we will vary the distance of the plant to the downstream water point of the Akosombo dam from zero to 100 km, calculate the LCOH at each 20 km and compare the values.

3.4.9 Carbon emission assessment

Each component of the energy system has a certain carbon footprint from raw material extraction to manufacturing, from its implementation to decommissioning. In this subsection,

we will evaluate the carbon emitted per kilowatt-hour of electricity produced et per kilogram of hydrogen produced.

$$CO_{2_{elect}}^{emission} = \frac{\sum_{i=pv,wind,battery} Elec_{prod}^{i} * CO_{2}{}_{factor}^{i}}{\sum_{i=pv,wind} Elec_{prod}^{i}} \quad 3.4\text{-}36$$

$$CO_{2_{H_2}}^{emission} = \frac{\sum_{i=comp} Output^{i} * CO_{2}{}_{factor}^{i}}{\sum_{i=comp} Output^{i}} \quad 3.4\text{-}37$$

3.4.10 Sensitivity analysis for LCOE and LCOH

Sensitivity analysis is a technique used to study the impact of variations in input parameters on the output of a model or system. There are several methods for conducting sensitivity analysis such as the One-at-a-Time (OAT) Analysis, Local Sensitivity Analysis (LSA), Global Sensitivity Analysis (GSA), etc. In this study, we will assume a variation of the parameters based on the global trend of RE and green hydrogen technologies. We will consider the same level of variation of the parameters in all the components of the energy systems; in other words, we will assume that the learning rate, the research and development (R&D), the cost reductions and external factors vary at the same order for all the considered components. In this analysis we will use the OAT method which consists of varying individually the input parameters while keeping all other parameters fixed at their baseline values; this way we identify how the parameters impact the LCOE and LCOH. The considered components and parameters are indexed in Appendix *1*.

4 Results and Discussion

4.1 Water cooling impact on the cell temperature and efficiency

The main difference between solar floating PV and solar land PV resides in the environmental conditions exposed to the solar PV modules. In opposite to solar land PV, floating PV benefits from the water-cooling effect underneath which lowers the cell temperature and increases the efficiency. Figure 4.1-1 shows the plots of the hourly cell temperature and efficiency of the two PV Systems LPV and FPV under similar meteorologic conditions calculated with the equations 3.4-7 and 3.4-9 individually integrated into the equation 3.4-6. As the figure shows, the cell temperature for LPV is greater than the one for floating. This is due to the water-cooling effect which brings down the module temperature allowing the PV module to operate at lower cell temperature. We can notice also that the seasonal variability has an impact also on the cell temperature. For instance, in the period of July to September which correspond to the raining season, the cell temperature of the floating

PV goes down at certain moment. This can be explained by the fact that the water temperature gets lower than usual due to the rain. But at the end of the period of October to December, the cell temperature of the floating PV and the one of land are quite similar. This period corresponds to the cold period. The ambient temperature gets lower and has the same impact on the land PV as well as on the floating PV.

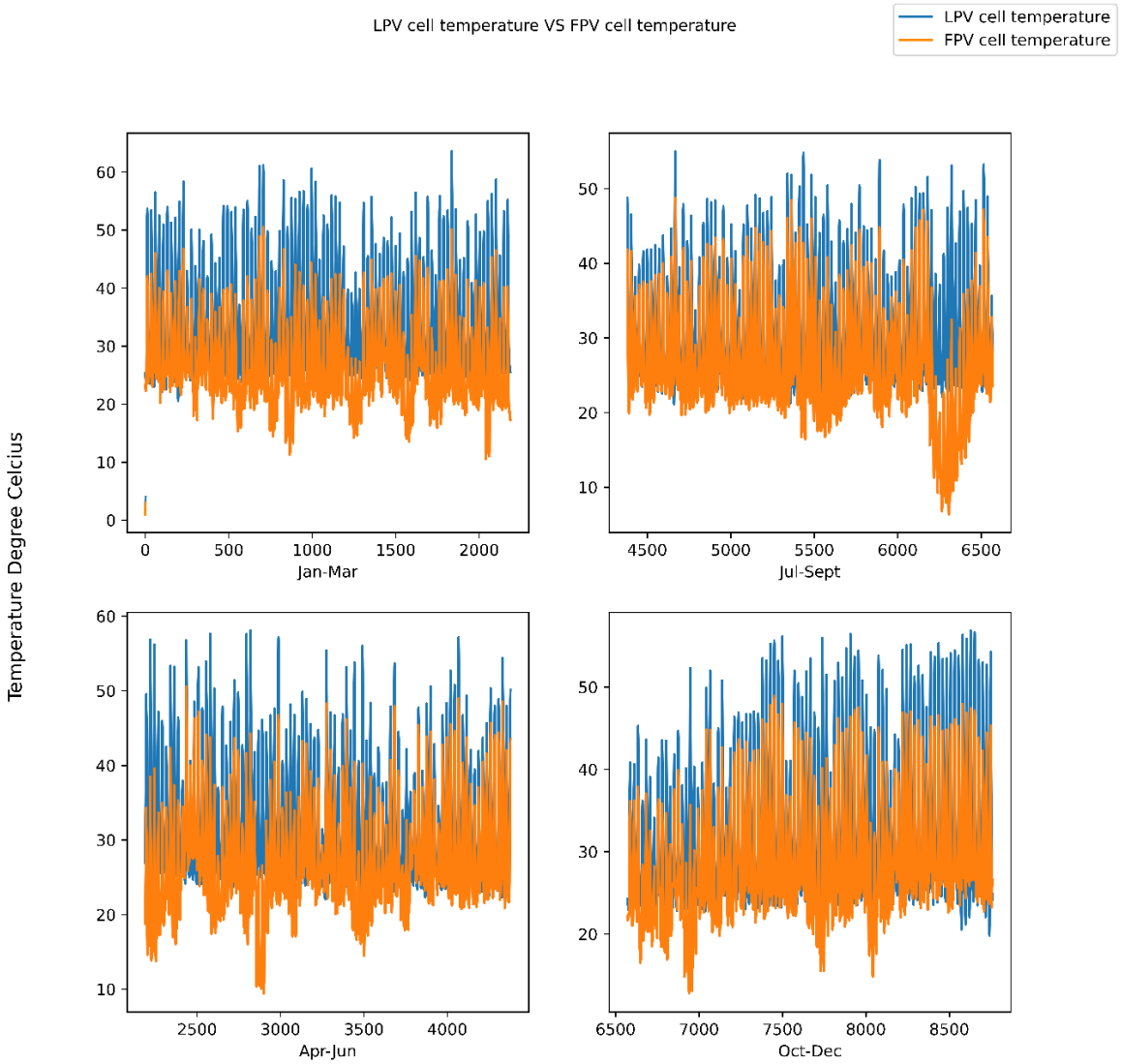

Figure 4.1-1: Cell temperature for Land PV and for Floating PV under the same conditions over the Volta Lake

4.2 Optimization results

4.2.1 Energy systems configurations

In the ESOF COMANDO, we have modelled four different energy systems: land PV energy system, floating PV energy system and combined land PV-Wind and floating PV-Wind energy systems. Each of these energy systems has three options: the alkaline electrolyser, the proton exchange membrane electrolyser and the solid oxide electrolyser to produce green

hydrogen. Each combination energy system-electrolyzer is optimized to produce 15 tons of green hydrogen daily and optionally inject any excess electricity. The results of the optimization are presented in Appendix *2* and Appendix *3*.

4.2.2 Energy systems optimisation

The optimization of the energy systems is done within the ESOF COMANDO with the Gurobi optimizer. The main outcomes of this optimization are the optimal total annualized costs (TACs), the optimal sizes of the components and the values of the operational variable.

4.2.2.1 Solar PV energy systems optimisation

The optimal results of energy systems comporting only PV as an electricity source are presented in Appendix *2*. The considered PV energy systems are optimized independently, therefore there is no correlation between the obtained results. However, all the energy systems have the same purpose: to provide fifteen tons of compressed green hydrogen. Depending on the technology and the costs implied, the results are different. In the table below, one can notice that the PV sizes for LPV and FPV are considerably higher when they are connected to the AEL or PEME than when they are connected to the SOEC. This is due to the difference in efficiencies (PEME=61.12%, AEL=68.1%, SOEC=83%). SOEC is more efficient than AEL and PEME, therefore, requests less electricity and less size to produce the demanded hydrogen. The battery storage is almost inexistent because there is no hydrogen demand during the night; moreover, the CapEx of the battery storage is much higher than the hydrogen storage. Therefore, by optimizing the costs hydrogen storage represents the better option. The total annualized costs are driven mostly by solar PV and the electrolyser.

4.2.2.2 Hybrid PV-Wind energy systems optimization

The hybrid energy systems PV-Wind are the LPV connected to wind turbines and FPV connected to wind turbines. The optimal results of these energy systems are listed in the table below. Like in the solar PV energy systems, the optimal solution doesn't include a battery storage

From Appendix *2* and Appendix *3*, one can notice that the energy system LPV coupled with alkaline electrolyser gives the lowest TACs whereas the FPV coupled with PEME gives the highest TACs. At this level, it is still impossible to determine which ES is the best option to produce green hydrogen. The LCOE and LCOH are the main deterministic parameters to identify the best option.

4.3 Levelized costs and carbon emission factors

4.3.1 Levelized cost of electricity

The LCOE is the average electricity cost that permits recovery of the total investments made over a considered financial lifetime of the plant. The LCOE is therefore calculated considering only the total costs of the PV plant and wind turbines over the total electricity produced.

Table 4.3-1: LCOE of all the considered energy systems

ES Configurations	**LPVA**	**LPVP**	**LPVS**	**FPVA**	**FPVP**	**FPVS**
LCOE [€/MWh]	61.194	61.193	61.194	64.274	64.28	64.277
ES Configurations	**LPVWA**	**LPVWP**	**LPVWS**	**FPVWA**	**FPVWP**	**FPVWS**
LCOE [€/MWh]	92.881	92.876	91.895	71.859	71.792	71.735

From Table 4.3-1, one can remark that the price of electricity produced from hybrid PV-Wind is greater than the one from only PV ES. This can be explained by the fact that the wind turbines are expensive compared to solar PV which affects the TACs of the hybrid ES. Moreover, the annual mean wind speed at Akosombo and Bonkoko is around 4.2m/s, which is relatively low to have a high electricity generation. The LPV ES gives the lowest LCOE which is about 61.19€/MWh followed by the FPV energy systems with around 64.27€/MWh. Around 92.8€/MWh is the highest LCOE given by the hybrid LPV-Wind ES.

4.3.2 Levelized cost of hydrogen

The LCOH calculation takes into consideration the total costs of the components involved in hydrogen production and the total electricity costs used to produce the green hydrogen.

Table 4.3-2: LCOH of all the considered energy systems

ES Configurations	**LPVA**	**LPVP**	**LPVS**	**FPVA**	**FPVP**	**FPVS**
LCOH [€/kgH_2]	5.926	7.581	7.245	6.038	7.676	7.456
ES Configurations	**LPVWA**	**LPVWP**	**LPVWS**	**FPVWA**	**FPVWP**	**FPVWS**
LCOH [€/kgH_2]	7.29	9.257	9.54	6.45	8.3	9.12

The lowest LCOH observed in the above table is 5.926 €/kgH_2, from the LPV with alkaline electrolyser followed by the FPV with alkaline electrolyser which has a value of 6.038 €/kgH_2. The highest LCOH is 9.54 €/kgH_2 given by the hybrid ES LPV-Wind. Despite

the water-cooling effect and the proximity of the water, the LCOH from FPV is slightly higher than the LCOH from LPV because the CapEx of FPV is around 13.34% higher than the one of LPV. This difference in cost could not be covered by the efficiency increase and the water proximity.

4.3.3 CO2 emission assessment

The components involved in green hydrogen production are not carbon-free. Each component has a carbon footprint which can be taken into consideration to evaluate the amount of carbon emitted per kilogrammes of green hydrogen produced. Table 4.3-3 shows the carbon emission factor of renewable electricity and green hydrogen.

Table 4.3-3: Carbon emissions factor of electricity and green hydrogen for all the considered energy systems

ES Configurations	**LPVA**	**LPVP**	**LPVS**	**FPVA**	**FPVP**	**FPVS**
Emissions per kgH_2 [g/kgH_2]	29.2	32.3	24.9	28.6	31.7	24.5
ES Configurations	**LPVWA**	**LPVWP**	**LPVWS**	**FPVWA**	**FPVWP**	**FPVWS**
Emissions per kgH_2 [g/kgH_2]	30.8	34.07	26.2	28.35	31.34	24.17

The values obtained ranged between 24.17 to 34.07 g/kgH_2 which are far below the threshold set to 1kgCO_2/kgH_2 by the Green Hydrogen Organisation (GH2, 2022). The hydrogen produced is therefore green.

4.4 Discussion

4.4.1 Impact of oxygen sales opportunity

Oxygen is a by-product of water electrolysis which can be necessary for other sectors such as healthcare centres, water treatment, and hydrogen fuel cell operation …. Therefore, oxygen has sales opportunities that can amortize the cost of green hydrogen. Assuming that the purpose of the plant is to produce oxygen, we determine the levelized cost of oxygen at the outlet of the electrolysers considering all the energy systems. The results are listed in the bellow table.

Table 4.4-1: Levelized cost of oxygen

ES Configurations	**LPVA**	**LPVP**	**LPVS**	**FPVA**	**FPVP**	**FPVS**
LCOH [€/kgH_2]	5.984	7.646	7.294	6.0939	7.739	7.494
LCOH* [€/kgH_2]	2.02	3.68	3.32	2.11	3.755	3.51
LCOO [€/kgO_2]	0.7541	0.9635	0.9188	0.7647	0.9711	0.9398

ES Configurations	$L_{PV}WA$	$L_{PV}WP$	$L_{PV}WS$	$F_{PV}WA$	$F_{PV}WP$	$F_{PV}WS$
LCOH [€/kgH_2]	7.343	9.316	9.59	6.494	8.364	9.17
LCOH* [€/kgH_2]	3.377	5.34	5.62	2.518	4.379	5.18
LCOO [€/kgO_2]	0.9257	1.174	1.21	0.816	1.05	1.15

LCOH is the cost of hydrogen if oxygen is sold at 0.5€/kgO_2*

Table 4.4-1 shows the cost of oxygen for each system at which the total costs of the hydrogen production plant are recovered after 25 years. The LCOO is ranged between 0.7541 to 1.21€/kgO2 at the outlet of the electrolyzer. These costs are far below what is found in the literature 2.631€/kgO_2 (Squadrito et al., 2018). In a case where the oxygen is sold at 0.5€/kgO_2, the LCOH could drop by 41.4% to 66.2% depending on the energy system. Selling hydrogen could consistently drop the green hydrogen cost.

4.4.2 Impact of water point proximity on the LCOH

The production of green hydrogen with a LPV system requires to access a water point which implies additional costs for water transfer and storage. As mentioned previously, the water access point in the downstream water of Akosombo Dam for both LPV and FPV. We assess how sensitive the LCOH is regarding the distance LPV-Waterpoint. Table 4.4-2 listed the different LCOH for LPV and hybrid LPV-Wind at 0, 50 and 100 km.

Table 4.4-2: Impact of distance between LPV plant and water access point on the LCOH

	Energy systems	$L_{PV}A$	$L_{PV}P$	$L_{PV}S$	$L_{PV}WA$	$L_{PV}WP$	$L_{PV}WS$
LCOH [€/kgH_2]	0 km	5.920795	7.57981	7.23979	7.2837	9.2488	9.5373
	50 km	5.92214	7.577335	7.24136	7.287029	9.25249	9.5410614
	100 km	5.926047	7.581237	7.24527	7.29072	9.255842	9.5443927

The results presented in the table show that the distance has a very slight impact on the LCOH as it increases about 0.02% to 0.1% per 100km.

4.4.3 Water savings

The natural phenomenon of water evaporation can lead to the loss of a considerable amount of essential water for reservoirs and water bodies. FPV has the asset to reduce this evaporated water over the area it covers. For each floating energy system configuration considered, we estimated the annual amount of water that could evaporate if an FPV system were not installed and assumed that the value found corresponded to the water saved. The

table below shows the annual water saved and the surface area covered by each FPV system during its operation.

Table 4.4-3: Surface area covered by FPV on the Volta Lake and water saved from evaporation

ES Configurations	$F_{PV}A$	$F_{PV}P$	$F_{PV}S$	$F_{PV}WA$	$F_{PV}WP$	$F_{PV}WS$
Surface area [km^{2}]	2.582	2.871	2.186	2.3843	2.672	2.052
Water savings [Mm^3/year]	7.65	8.506	6.478	7.064	7.916	6.08

From the above table, one can observe the benefit of FPV on water losses due to evaporation. With FPV which covers 2.052 to 2.871 km^2 of the Volta Lake an estimated amount of 6.08 to 8.506 million cubic meters of water can be saved from evaporation per year. The surface area covered represents only 0.024 % to 0.034% of the total surface area of Volta Lake.

4.4.4 Sensitivity analysis

Sensitivity analysis is a method used to assess how the change of an input parameter could impact the outcome of a model or simulation. The sensitivity analysis in this work is focused on the parameters of the key components of the energy system.

4.4.4.1 Impact of discount rate

The nominal discount rate is the measure of the time value of the cost of money; in other words, it is a financial concept used to determine the present value of future cash flows. It is the rate at which future cash flows are discounted back to their equivalent value in today's terms. The discount rate is an important parameter to be considered in a project implementation because it is highly dependent on several factors (investor’s rate of return, risk premium, planning horizon, interest rates, and income and property taxes) (Short et al., 1995). It changes from country to country, from industry to industry and company to company. The analysis is done at 4% and 10% of the normal discount rate and the results are summarised in the following tables.

Table 4.4-4: Sensitivity analysis: LCOE and LCOH at 4% of discount rate

	ES Configurations	$L_{PV}A$	$L_{PV}P$	$L_{PV}S$	$F_{PV}A$	$F_{PV}P$	$F_{PV}S$
Analysis results	**LCOE [€/MWh]**	45.8328	45.8327	45.833	47.3186	47.3186	47.3186
	LCOH [€/kgH_2]	4.529	5.8618	5.615	4.5666	5.885	5.688
	ES Configurations	$L_{PV}WA$	$L_{PV}WP$	$L_{PV}WS$	$F_{PV}WA$	$F_{PV}WP$	$F_{PV}WS$

Analysis results	**LCOE [€/MWh]**	71.177	71.116	70.397	53.5856	53.5856	53.537
	LCOH [€/kgH_2]	5.584	7.122	7.355	4.812	6.3327	6.979

The results of the analysis presented in Table 4.4-4 and Table 4.4-5 show that the discount rate has a key place in project investment. The discount rate of 4% decreases the baseline LCOH by 22.9% to 25.4% while the discount rate of 10% increases the baseline LCOH by 19.2% to 20.%. To have a cost-competitive green hydrogen, the lower the discount rate the smaller the LCOH.

Table 4.4-5:Sensitivity analysis: LCOE and LCOH at 10% of normal discount rate

	ES Configurations	**$L_{PV}A$**	**$L_{PV}P$**	**$L_{PV}S$**	**$F_{PV}A$**	**$F_{PV}P$**	**$F_{PV}S$**
Analysis results	**LCOE [€/MWh]**	74.319	74.3195	74.3199	78.7664	78.766	78.7664
	LCOH [€/kgH_2]	7.11	9.0372	8.625	7.285	9.1989	8.9034
	ES Configurations	**$L_{PV}WA$**	**$L_{PV}WP$**	**$L_{PV}WS$**	**$F_{PV}WA$**	**$F_{PV}WP$**	**$F_{PV}WS$**
Analysis results	**LCOE [€/MWh]**	111.4034	111.404	110.262	87.414	87.34466	87.278
	LCOH [€/kgH_2]	8.740	11.05	11.405	7.797	9.982	10.9538

4.4.4.2 Impact of the lifetime variations

- **Land PV lifetime**

The baseline lifetime of the LPV is 30 years. We will assume this value is the maximum a LPV can last because of the temperature effect which accelerates the degradation rate. Worst cases are only considered in this analysis, for instance, 20- and 25-year lifetime.

Table 4.4-6: Sensitivity analysis: LCOE and LCOH for LPV lifetime at 20 years

	ES Configurations	**$L_{PV}A$**	**$L_{PV}P$**	**$L_{PV}S$**	**$L_{PV}WA$**	**$L_{PV}WP$**	**$L_{PV}WS$**
Analysis results	**LCOE [€/MWh]**	69.1642	69.1640	69.1644	99.7798	99.7808	99.7071
	LCOH [€/kgH_2]	6.335	8.025	7.582	7.636	9.639	10.05

Table 4.4-7: Sensitivity analysis: LCOE and LCOH for LPV lifetime at 25 years

	ES Configurations	**$L_{PV}A$**	**$L_{PV}P$**	**$L_{PV}S$**	**$L_{PV}WA$**	**$L_{PV}WP$**	**$L_{PV}WS$**
Analysis results	**LCOE [€/MWh]**	64.191	64.191	64.191	95.473	95.474	94.510

	LCOH [€/kgH_2]	6.0738	7.745	7.369	7.418	9.398	9.652

The lifetime of the LPV has an impact on the LCOE and LCOH. From the baseline, the FPV has a 30-year operation lifetime, however, a LPV can be subjected to high temperatures which can reduce the lifetime of the solar PV modules. A five-year lifetime reduction can lead to an increase of 1.17% to 2.5% of the LCOH and an increase of 2.8% to 4.9% of the LCOE. Good and regular maintenance is the best solution to maintain and even extend the lifetime of solar PV modules.

- **Floating PV lifetime**

The baseline lifetime of the LPV is 30 years. Two additional cases are considered for this parameter of the FPV: a worst case of 25 years lifetime for unexpected external factors that could happen and a good case of 35 years assuming that the water-cooling effect decreases the ageing rate of the FPV modules.

Table 4.4-8: Sensitivity analysis: LCOE and LCOH for FPV lifetime at 25 years

	ES Configurations	**F_{PV}A**	**F_{PV}P**	**F_{PV}S**	**F_{PV}WA**	**F_{PV}WP**	**F_{PV}WS**
Analysis results	**LCOE [€/MWh]**	67.585	67.5857	67.5857	74.8385	74.779	74.724
	LCOH [€/kgH_2]	6.20	7.861	7.589	6.6	8.47	9.252

Table 4.4-9: Sensitivity analysis: LCOE and LCOH for FPV lifetime at 35 years

	ES Configurations	**F_{PV}A**	**F_{PV}P**	**F_{PV}S**	**F_{PV}WA**	**F_{PV}WP**	**F_{PV}WS**
Analysis results	**LCOE [€/MWh]**	62.177	62.177	62.177	69.897	69.897	69.84
	LCOH [€/kgH_2]	5.93	7.557	7.295	6.27	8.196	9.04

From Table 4.4-9, we can deduce that the extension of the FPV lifetime can decrease the LCOE by 2.64% to 3.27% and the LCOH by 0.8% to 2.79%. Due to the water-cooling effect on the FPV, it is expected to have a lifetime extension.

- **Wind turbines lifetime**

The normal lifetime of the wind turbine is 25 years. For uncertainty and probable improvements, we assume 20 years as the worst case and 30 years for the good case.

Table 4.4-10: Sensitivity analysis: LCOE and LCOH for Wind turbine lifetime at 20 years

	ES Configurations	**L_{PV}WA**	**L_{PV}WP**	**L_{PV}WS**	**F_{PV}WA**	**F_{PV}WP**	**F_{PV}WS**

Analysis results	**LCOE [€/MWh]**	95.715	95.715	94.651	72.842	72.7728	72.706
	LCOH [€/kgH_2]	7.43	9.41	9.6587	6.498	8.357	9.166

Table 4.4-11: Sensitivity analysis: LCOE and LCOH for Wind turbine lifetime at 30 years

	ES Configurations	**L_{PV}WA**	**L_{PV}WP**	**L_{PV}WS**	**F_{PV}WA**	**F_{PV}WP**	**F_{PV}WS**
Analysis results	**LCOE [€/MWh]**	91.16	91.167	90.244	71.258	71.2	71.15
	LCOH [€/kgH_2]	7.2	9.156	9.47	6.418	8.27	9.1

Table 4.4-10 and Table 4.4-11 above present the impact of the wind turbine lifetime variation on the LCOE and LCOH. The difference in cost is low since the optimal sizes in all the hybrid ES are not too much. For 25 years of lifetime, the LCOE and LCOH increase by 1.35% to 3% and 0.5% to 1.92% respectively, while for a lifetime of 30 years, they decrease by 0.82% to 1.85% and 0.22% to 1.23% respectively.

- **Electrolyzer lifetime**

  For all the considered electrolysers, we assume -10% and +10% of their respective normal lifetime respectively for the worst case and good case.

Table 4.4-12: Sensitivity analysis: LCOE and LCOH for 10% less the baseline lifetime of all electrolysers

	ES Configurations	**L_{PV}A**	**L_{PV}P**	**L_{PV}S**	**F_{PV}A**	**F_{PV}P**	**F_{PV}S**
Analysis results	**LCOE [€/MWh]**	61.194	61.194	61.194	64.27	64.276	64.276
	LCOH [€/kgH_2]	6.02	7.74	7.42	6.135	7.837	7.565
	ES Configurations	**L_{PV}WA**	**L_{PV}WP**	**L_{PV}WS**	**F_{PV}WA**	**F_{PV}WP**	**F_{PV}WS**
Analysis results	**LCOE [€/MWh]**	92.877	92.8	91.9	71.79	71.792	71.73
	LCOH [€/kgH_2]	7.366	9.37	9.73	6.457	8.45	9.328

Table 4.4-13: Sensitivity analysis: LCOE and LCOH for 10% more the baseline lifetime of all electrolysers

	ES Configurations	**L_{PV}A**	**L_{PV}P**	**L_{PV}S**	**F_{PV}A**	**F_{PV}P**	**F_{PV}S**
Analysis results	**LCOE [€/MWh]**	61.194	61.194	61.194	64.276	64.276	64.276
	LCOH [€/kgH_2]	5.84	7.446	7.1	5.96	7.54	7.3
	ES Configurations	**L_{PV}WA**	**L_{PV}WP**	**L_{PV}WS**	**F_{PV}WA**	**F_{PV}WP**	**F_{PV}WS**

Analysis results	**LCOE [€/MWh]**	92.877	92.877	91.90	71.85	71.79	71.734
	LCOH [€/kgH_2]	7.226	9.142	9.39	6.38	8.186	8.96

The lifetime of the electrolyser stack can have a big impact on the LCOH because the shorter the lifetime, the more replacement occurs which implies additional costs. Assuming a decrease and an increase of 10% of the actual lifetime of the considered electrolysers, it is deductible from the sensitivity analysis that a 10% reduction of the lifetime can lead to an increase by 0.1% to 2.4% of the LCOH, while an increase of 10% of the lifetime decreases the LCOH by 0.8% to 2.1%. Future trends show an increase in the learning rate of the electrolyser technology meaning that green hydrogen could be more affordable with the technology improvements.

4.4.4.3 Impact of efficiency electrolyser's efficiency variations

The sensitivity values for this analysis are -10% (worst case) and +10% (good case) of the baseline reference efficiency of the electrolysers.

Table 4.4-14: Sensitivity analysis: LCOH for -10% and +10% of the reference efficiency of the electrolysers

	ES Configurations	**LPVA**	**LPVP**	**LPVS**	**FPVA**	**FPVP**	**FPVS**
Worst case (-10%)	**LCOH [€/kgH_2]**	6.55	8.394	8.02	6.68	8.5	8.174
Good case (+10%)	**LCOH [€/kgH_2]**	5.4	6.90	6.6	5.5	7	6.8

The efficiency of the electrolyser also has to be considered in a green hydrogen production plant implementation and operation. The lower the efficiency the more the hydrogen is expensive. By considering a range of -10% and +10% of the actual efficiency, we assess the impact on the LCOH. With an increase of 10% of the actual efficiency for all the electrolysers, the LCOH decreases by 8.8% while decreasing by 10% the LCOH increases by around 10% for all the electrolysers.

4.4.4.4 Impact of Component Cost Variations

In this part, we are assessing how the change in the total installed costs (TICs) of the components such as the LPV, FPV and electrolysers affect the LCOE and LCOH. We assumed +10% (worst case) and -10% (good case) variations of the baseline TICs firstly for the LPV, FPV and electrolysers and secondly for the whole hydrogen production plant.

Table 4.4-15: Sensitivity analysis: LCOH for -10% and +10% of the TICs of PV systems and electrolysers

	ES Configurations	$L_{PV}A$	$L_{PV}P$	$L_{PV}S$	$F_{PV}A$	$F_{PV}P$	$F_{PV}S$
Worst case (+10%)	**LCOE [€/MWh]**	67.313	67.313	67.313	70.704	70.704	70.704
	LCOH [€/kgH_2]	6.50	8.32	7.95	6.62	8.42	8.18
Good case (-10%)	**LCOE [€/MWh]**	57.41	57.41	57.41	59.774	59.774	59.774
	LCOH [€/kgH_2]	5.46	6.96	6.96	5.539	7.025	6.796

If 10% of the TICs in added up to the actual TICs, the LCOE and LCOH increase by around 10%. In the case that 10% of the TICs are reduced, the LCOE and LCOH decrease by 6.18% to 7% and 4% to 8.8% respectively. A large deployment of green hydrogen utilities could impact the TICs of the hydrogen production plant leading to a decrease in the price of green hydrogen

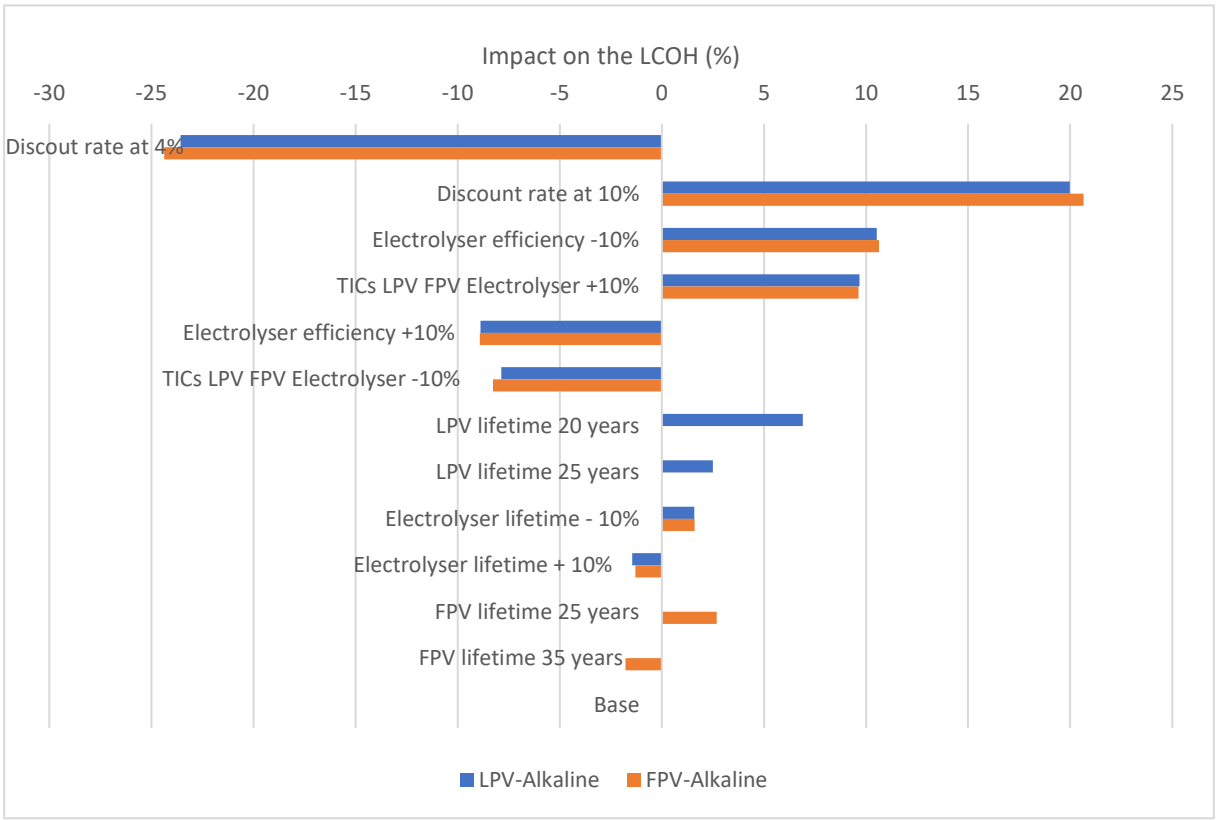

Figure 4.4-1: Sensitivity analysis of some parameters on the LCOH

Among the parameters considered in the sensitivity analysis, the above figure shows that the parameters that impact the most the LCOH are the discount rate, the efficiency of the electrolysers, and the TICs of the PV systems and the electrolysers. Projects with lower

discount rates can give lower LCOH and vice versa. Furthermore, with the increase of the technologies' learning rate, the efficiency is expected to increase while the TICs decrease. The price of hydrogen will get lower and lower as the technology improvements are going further.

5 Conclusions and recommendations

In the context of climate change, energy crisis and energy transition, green hydrogen has been identified as a potential solution. However, green hydrogen production is expensive due to several reasons: expensive green hydrogen production utilities, expensive renewable electricity, expensive access to sustainable water, the intermittency of solar and wind energy sources and the impact of weather conditions. Therefore, this work aims to design a techno-economic optimization model that minimizes the green hydrogen production costs taking in consideration the weather conditions and water availability of the location. The model has been built within the COMANDO ESOF using the Python programming language and solved with the Gurobi optimizer. It is a relevant model as it can help and support the decision-makers.

Through a comprehensive exploration of several energy systems with different electrolyser technologies, we have gained valuable insights into the optimal energy system configuration that gives a lower LCOE and LCOH. The energy systems considered in our techno-economical optimization model are LPV and FPV, hybrid LPV-Wind and FPV-Wind, each of them connected either to an alkaline electrolyser, a proton exchange membrane electrolyser or a solid oxide electrolysis cell. The results of the optimization of all the systems give LCOE which are ranged from 61.19 €/MWh to 92.88€/MWh depending on the energy systems. The LPV gives a LCOE of 61.19€/MWh which is lower than 64.274€/MWh corresponding to the LCOE of FPV. Regarding the cost of hydrogen, the LPV and FPV with alkaline electrolyser give costs which are in the same range: 5.926€/kgH_2 and 6.038€/kgH_2 respectively. These costs obtained are following those found in the literature. However, by considering the option to sell the by-product oxygen at only 0.5€/kgO_2, the LCOH could drop by 41.4% to 66.2% depending on the energy system reaching 2.02€/kgH_2 to 5.62€/kgH_2. If the cost of oxygen is set higher than 0.5€/kgO_2, the LCOH could get lesser. Furthermore, we evaluated the carbon emission per kilogram of hydrogen produced and got values ranging between 24.17 to 34.07 g/kgH_2 which are far below the threshold set to 1kgCO_2/kgH_2 by the Green Hydrogen Organisation (GH2, 2022). Regarding the impact of the water proximity to

the LPV, we found that the distance has a very slight impact on the LCOH as it increases from about 0.02% to 0.1% per 100km. For a FPV, we evaluated the water savings from evaporation and found that 2.871 km^2 of the Volta Lake covered by FPV, an estimated amount of 6.08 to 8.506 million cubic meters of water can be saved from evaporation per year.

We undertook sensitivity analysis to determine how impactful are some parameters on the LCOH. We found that the discount rate has a high impact on the LCOH, the higher the discount rate, the higher the LCOH and vice versa. Regarding the lifetime of the components, the results show that if the lifetime is high, the LCOH decreases while it increases if the lifetime gets lower. The same applies to the LCOE if the component is a renewable electricity generator. The efficiency of the components also impacts the LCOH, for instance for the electrolysers, with an increase of 10% of the actual efficiency, the LCOH decreases by 8.8% while decreasing by 10% the LCOH increases by around 10% for all the electrolysers. In the same case, the TICs of the components impact the LCOE and the LCOH. In this study, we assumed a 10% increase and decrease in the LPV, the FPV and the electrolysers. We found a 10% increase in the LCOE and LCOH if the costs are increased by 10% and for a 10% decrease in the TICs, we observed a decrease of 6.18% to 7% and 4% to 8.8% of the LCOE and LCOH respectively.

Our study reveals that the FPV gives a higher efficiency compared to the LPV due to the water-cooling effect. Additionally, the lowest LCOH is given an alkaline electrolyser powered by LPV which gives the lowest LCOE, followed by the FPV with a slight difference of 0.112€. Both LCOHs are cost-competitive and could be more if the oxygen is sold. Our initial hypothesis on the water-cooling effect has been confirmed unlike the ones concerning the LCOE and LCOH. This is due to the high difference in TICs between FPV and LPV. In the case that the TICs of the FPV are the same as the TICs of the LPV, the LCOE becomes 57.95€/kWh and the LCOH 5.72€/kgH_2 which is lower than the base case results.

Furthermore, this study has contributed to the existing body of knowledge by giving more accuracy on the techno-economic analysis, and the flexibility to choose among several energy systems the most cost-competitive configuration which gives the lowest LCOH depending on the location.

After a deep analysis of the different results we got, we could suggest the different actors and stakeholders to investigate more on the green hydrogen production using floating PV. As a matter of fact, many factors such as the water proximity, the water accessibility, the water-cooling effect, the water savings, the land saving etc are very impactful on the floating PV electricity production as well as the hydrogen production. The green hydrogen produced

from floating PV can therefore get lower price and be more competitive with the other hydrogen. In addition, we can suggest to undertake a specific study focused on green hydrogen production assessment on all the existent water body in West Africa. Furthermore, an increasing of the learning level of floating PV could decrease considerably the total installation costs of the floating PV which is higher than the land PV.

However, it is important to acknowledge certain limitations of this study, such as the integration of the AC and DC power flows in the model as well as the hydrogen flow network, and the accuracy and current of the costs. These limitations provide avenues for future research to delve deeper into the optimization of green hydrogen production plants including all the power networks involved.

BIBLIOGRAPHY

ABB. (2021). *Lithium-ion battery system for ABB UPS solutions-SDI CE & UL 9540 Reliable, lightweight and compact UPS energy storage for critical applications*.

Akhsassi, M., El Fathi, A., Erraissi, N., Aarich, N., Bennouna, A., Raoufi, M., & Outzourhit, A. (2018). Experimental investigation and modeling of the thermal behavior of a solar PV module. *Solar Energy Materials and Solar Cells*, *180*, 271–279. https://doi.org/10.1016/j.solmat.2017.06.052

Barwe, S., De Pauw; • Bp, M., Andrews, A., Becker, H., Fernandez, B., Oci, ; •, & Raeymaekers, F. (2023). *Next Level Solid Oxide Electrolysis*. https://ispt.eu/media/20230508-FINAL-SOE-public-report-ISPT.pdf

Batalla-Bejerano, J., & Trujillo-Baute, E. (2016). Impacts of intermittent renewable generation on electricity system costs. *Energy Policy*, *94*, 411–420. https://doi.org/10.1016/j.enpol.2015.10.024

Becker, H., Murawski, J., Shinde, D. V., Stephens, I. E. L., Hinds, G., & Smith, G. (2023). Impact of impurities on water electrolysis: a review. In *Sustainable Energy and Fuels* (Vol. 7, Issue 7, pp. 1565–1603). Royal Society of Chemistry. https://doi.org/10.1039/d2se01517j

Bhandari, R. (2022). Green hydrogen production potential in West Africa – Case of Niger. *Renewable Energy*, *196*, 800–811. https://doi.org/10.1016/j.renene.2022.07.052

Bhandari, R., Kumar, B., & Mayer, F. (2020). Life cycle greenhouse gas emission from wind farms in reference to turbine sizes and capacity factors. *Journal of Cleaner Production*, *277*, 123385. https://doi.org/10.1016/j.jclepro.2020.123385

Bonkaney, A. L., Madougou, S., & Adamou, R. (2017). Impact of Climatic Parameters on the Performance of Solar Photovoltaic (PV) Module in Niamey. *Smart Grid and Renewable Energy*, *08*(12), 379–393. https://doi.org/10.4236/sgre.2017.812025

Bouraiou, A., Hamouda, M., Chaker, A., Mostefaoui, M., Lachtar, S., Sadok, M., Boutasseta, N., Othmani, M., & Issam, A. (2015). Analysis and evaluation of the impact of climatic conditions on the photovoltaic modules performance in the desert environment. *Energy Conversion and Management*, *106*, 1345–1355. https://doi.org/10.1016/j.enconman.2015.10.073

Buttler, A., & Spliethoff, H. (2018). Current status of water electrolysis for energy storage, grid balancing and sector coupling via power-to-gas and power-to-liquids: A review. In

Renewable and Sustainable Energy Reviews (Vol. 82, pp. 2440–2454). Elsevier Ltd. https://doi.org/10.1016/j.rser.2017.09.003

C3S-CDS. (2020). Lake surface water temperature from 1995 to present derived from satellite observation. In *Copernicus Climate Change Service (C3S) Climate Data Store (CDS)*. https://doi.org/https://doi.org/10.24381/cds.d36187ac

Caldera, U., Bogdanov, D., & Breyer, C. (2018). Desalination Costs Using Renewable Energy Technologies. In *Renewable Energy Powered Desalination Handbook* (pp. 287–329). Elsevier. https://doi.org/10.1016/B978-0-12-815244-7.00008-8

Charles, L. K. W., Lim, J., Won, C., & Ahn, H. (2018). Prediction Model of Photovoltaic Module Temperature for Power Performance of Floating PVs. *Energies*, *11*(2), 447. https://doi.org/10.3390/en11020447

Clark, R. M., Selvakumar, A., Sivaganesan, M., Selvakumar, ; Ari, & Sethi, V. (2002). Costs Models for Water Supply Distribution Systems Cost Models for Water Supply Distribution Systems. *Article in Journal of Water Resources Planning and Management*. https://doi.org/10.1061/ASCE0733-94962002128:5312

COMANDO Repository. (2021). *COMANDO Repository*. https://jugit.fz-juelich.de/iek-10/public/optimization/comando

Dewi, T., Risma, P., & Oktarina, Y. (2019). A Review of Factors Affecting the Efficiency and Output of a PV System Applied in Tropical Climate. *IOP Conference Series: Earth and Environmental Science*, *258*(1). https://doi.org/10.1088/1755-1315/258/1/012039

Divya Mittal, Bharat Kumar Saxena, & K. V. S. Rao. (2017). *Comparison of Floating Photovoltaic Plant with Solar Photovoltaic Plant for Energy Generation at Jodhpur in India*. IEEE.

Quotation - 2000LPH Ultrapure water treatment Plant, (2023).

Consumable table - 2000LPH Ultrapure water treatment Plant, (2023).

Dörenkämper, M., Wahed, A., Kumar, A., de Jong, M., Kroon, J., & Reindl, T. (2021). The cooling effect of floating PV in two different climate zones: A comparison of field test data from the Netherlands and Singapore. *Solar Energy*, *219*, 15–23. https://doi.org/10.1016/j.solener.2021.03.051

Dubey, S., Sarvaiya, J. N., & Seshadri, B. (2013). Temperature dependent photovoltaic (PV) efficiency and its effect on PV production in the world - A review. *Energy Procedia*, *33*, 311–321. https://doi.org/10.1016/j.egypro.2013.05.072

EIA. (2022). *Levelized Costs of New Generation Resources in the Annual Energy Outlook 2022*.

Elberry, A. M., Thakur, J., Santasalo-Aarnio, A., & Larmi, M. (2021). Large-scale compressed hydrogen storage as part of renewable electricity storage systems. *International Journal of Hydrogen Energy*, *46*(29), 15671–15690. https://doi.org/10.1016/j.ijhydene.2021.02.080

Escamilla, A., Sánchez, D., & García-Rodríguez, L. (2022). Assessment of power-to-power renewable energy storage based on the smart integration of hydrogen and micro gas turbine technologies. *International Journal of Hydrogen Energy*, *47*(40), 17505–17525. https://doi.org/10.1016/j.ijhydene.2022.03.238

Francesco Pavan, Jose M Bermudez, Stavroula Evangelopoulou, & Simon Bennett. (2023, July 10). *Electrolysers - Energy System - IEA*. Electrolysers - Energy System - IEA. https://www.iea.org/energy-system/low-emission-fuels/electrolysers

Green Hydrogen Organization. (2022). *The Green Hydrogen Standard*. www.gh2.org

Gökçek, M., & Kale, C. (2018). Optimal design of a Hydrogen Refuelling Station (HRFS) powered by Hybrid Power System. *Energy Conversion and Management*, *161*, 215–224. https://doi.org/10.1016/j.enconman.2018.02.007

Gonzalez Sanchez, R., Kougias, I., Moner-Girona, M., Fahl, F., & Jäger-Waldau, A. (2021). Assessment of floating solar photovoltaics potential in existing hydropower reservoirs in Africa. *Renewable Energy*, *169*, 687–699. https://doi.org/10.1016/j.renene.2021.01.041

Gorre, J., Ruoss, F., Karjunen, H., Schaffert, J., & Tynjälä, T. (2020a). Cost benefits of optimizing hydrogen storage and methanation capacities for Power-to-Gas plants in dynamic operation. *Applied Energy*, *257*. https://doi.org/10.1016/j.apenergy.2019.113967

Gorre, J., Ruoss, F., Karjunen, H., Schaffert, J., & Tynjälä, T. (2020b). Cost benefits of optimizing hydrogen storage and methanation capacities for Power-to-Gas plants in dynamic operation. *Applied Energy*, *257*. https://doi.org/10.1016/j.apenergy.2019.113967

Goswami, A., Sadhu, P., Goswami, U., & Sadhu, P. K. (2019). Floating solar power plant for sustainable development: A techno-economic analysis. *Environmental Progress and Sustainable Energy*, *38*(6). https://doi.org/10.1002/ep.13268

GSA. (2023a). *Bonkoko's solar potential*. https://globalsolaratlas.info/map?c=6.28834,-0.217667,11&s=6.287999,-0.218079&m=site

GSA. (2023b). *Volta Lake's solar potential*. https://globalsolaratlas.info/detail?c=6.489955,-0.000041,11&s=6.489955,-0.000041&m=site&pv=hydro,180,10,1000

Gurfude, S. S., Bhavitha, C., Tanusha, D., Mounika, D., Gouda Kake, S. P., Saisudha, M., & Kulkarni, P. S. (2020, September 25). Techno-economic Analysis of 1 MWp Floating Solar PV Plant. *Proceedings of 2020 IEEE 1st International Conference on Smart*

Technologies for Power, Energy and Control, STPEC 2020. https://doi.org/10.1109/STPEC49749.2020.9297740

GWA. (2023a, June). *Global Wind Atlas- Akosombo*. https://globalwindatlas.info/en

GWA. (2023b, June). *Global Wind Atlas- Bonkoko*. https://globalwindatlas.info/en

Harboe, S., Schreiber, A., Margaritis, N., Blum, L., Guillon, O., & Menzler, N. H. (2020). Manufacturing cost model for planar 5 kWel SOFC stacks at Forschungszentrum Jülich. *International Journal of Hydrogen Energy*, *45*(15), 8015–8030. https://doi.org/10.1016/j.ijhydene.2020.01.082

Hassan, Q., Abdulrahman, I. S., Salman, H. M., Olapade, O. T., & Jaszczur, M. (2023). Techno-Economic Assessment of Green Hydrogen Production by an Off-Grid Photovoltaic Energy System. *Energies*, *16*(2). https://doi.org/10.3390/en16020744

Hydrogen Council. (2020). *Path to hydrogen competitiveness A cost perspective*. www.hydrogencouncil.com.

IEA. (2019). *The Future of Hydrogen*.

IEA. (2020, September 24). *IEA, Global average levelised cost of hydrogen production by energy source and technology, 2019 and 2050, IEA, Paris*. IEA. https://www.iea.org/data-and-statistics/charts/global-average-levelised-cost-of-hydrogen-production-by-energy-source-and-technology-2019-and-2050

IEA. (2022a). *Global Hydrogen Review 2022*. www.iea.org/t&c/

IEA. (2022b). *Renewables 2022*. www.iea.org

IPCC-AR6. (2023). Synthesis reportof the ipcc sixth assessment report (AR6). In *Diriba Korecha Dadi*. Panmao Zhai. https://www.ipcc.ch/report/sixth-assessment-report-cycle/#report-chapters

IRENA. (2022a). *Global hydrogen trade to meet the 1.5°c climate goal part i trade outlook for 2050 and way forward* (International Renewable Energy Agency, Ed.). International Renewable Energy Agency. www.irena.org/publications

IRENA. (2022b). *Renewable power generation costs in 2021*. www.irena.org

ISPT. (2020). *Gigawatt green hydrogen plant*. https://ec.europa.eu/commission/presscorner/detail/en/ip_20_1259

Josué, N. L. (2013). *Comparing the calculated coefficients of performance of a class of wind turbines that produce power between 330 kW and 7,500 kW*.

Khan, M. A., Al-Shankiti, I., Ziani, A., & Idriss, H. (2021). Demonstration of green hydrogen production using solar energy at 28% efficiency and evaluation of its economic viability. *Sustainable Energy and Fuels*, *5*(4), 1085–1094. https://doi.org/10.1039/d0se01761b

King, D. L., Boyson, W. E., & Kratochvil, J. A. (2004). *PHOTOVOLTAIC ARRAY PERFORMANCE MODEL*.

Kjeldstad, T., Lindholm, D., Marstein, E., & Selj, J. (2021). Cooling of floating photovoltaics and the importance of water temperature. *Solar Energy*, *218*, 544–551. https://doi.org/10.1016/j.solener.2021.03.022

Langiu, M., Shu, D. Y., Baader, F. J., Hering, D., Bau, U., Xhonneux, A., Müller, D., Bardow, A., Mitsos, A., & Dahmen, M. (2021). COMANDO: A Next-Generation Open-Source Framework for Energy Systems Optimization. *Computers and Chemical Engineering*, *152*. https://doi.org/10.1016/J.COMPCHEMENG.2021.107366

Leow, W. Z., Irwan, Y. M., Irwanto, M., Amelia, A. R., & Safwati, I. (2019). Influence of wind speed on the performance of photovoltaic panel. *Indonesian Journal of Electrical Engineering and Computer Science*, *15*(1), 60–68. https://doi.org/10.11591/ijeecs.v15.i1.pp60-68

Liu, L., Wang, Q., Lin, H., Li, H., Sun, Q., & Wennersten, R. (2017). Power Generation Efficiency and Prospects of Floating Photovoltaic Systems. *Energy Procedia*, *105*, 1136–1142. https://doi.org/10.1016/j.egypro.2017.03.483

Martinus, G. de K., & Venter, W. C. (2017). Power calculation accuracy as a function of wind data resolution. *Journal of Energy in Southern Africa*, *28*(2), 71–84. https://doi.org/10.17159/2413-3051/2017/v28i2a1656

Mattei, M., Notton, G., Cristofari, C., Muselli, M., & Poggi, P. (2006). Calculation of the polycrystalline PV module temperature using a simple method of energy balance. *Renewable Energy*, *31*(4), 553–567. https://doi.org/10.1016/j.renene.2005.03.010

National Geographic Society. (2023, June 19). *Renewable Resources*. https://education.nationalgeographic.org/resource/renewable-resources/

Niyaz, H. M., Kumar, M., & Gupta, R. (2021). Estimation of module temperature for water-based photovoltaic systems. *Journal of Renewable and Sustainable Energy*, *13*(5). https://doi.org/10.1063/5.0059794

NREL. (2012). Life Cycle Greenhouse Gas Emissions. *U.S. Department of Energy, Office of Energy Efficiency and Renewable Energy*.

NREL. (2022, July 21). *Utility-Scale Battery Storage | Electricity | 2022 | ATB | NREL*. NREL. https://atb.nrel.gov/electricity/2022/utility-scale_battery_storage#QASDZMI6

Omran, M. G. H., Engelbrecht, A. P., & Salman, A. (2007). An overview of clustering methods. In *Intelligent Data Analysis* (Vol. 11, Issue 6, pp. 583–605). IOS Press. https://doi.org/10.3233/ida-2007-11602

Osei, L. K., Asmah, R., Aikins, S., & Karikari, A. Y. (2019). Effects of Fish Cage Culture on Water and Sediment Quality in the Gorge Area of Lake Volta in Ghana: A Case Study of Lee Fish Cage Farm. *Ghana Journal of Science*, *60*(1), 1–16. https://doi.org/10.4314/gjs.v60i1.1

Osman, A. I., Chen, L., Yang, M., Msigwa, G., Farghali, M., Fawzy, S., Rooney, D. W., & Yap, P. S. (2022). Cost, environmental impact, and resilience of renewable energy under a changing climate: a review. *Environmental Chemistry Letters*, 741–764. https://doi.org/10.1007/s10311-022-01532-8

Pfenninger, S., & Staffell, I. (2016). Long-term patterns of European PV output using 30 years of validated hourly reanalysis and satellite data. *Energy*, *114*, 1251–1265. https://doi.org/10.1016/j.energy.2016.08.060

Rabiee, A., Keane, A., & Soroudi, A. (2021). Green hydrogen: A new flexibility source for security constrained scheduling of power systems with renewable energies. *International Journal of Hydrogen Energy*, *46*(37), 19270–19284. https://doi.org/10.1016/j.ijhydene.2021.03.080

Rahaman, M. A., Chambers, T. L., Fekih, A., Wiecheteck, G., Carranza, G., & Possetti, G. R. C. (2023). Floating photovoltaic module temperature estimation: Modeling and comparison. *Renewable Energy*, *208*, 162–180. https://doi.org/10.1016/j.renene.2023.03.076

Ramasamy, V., Feldman, D., Desai, J., & Margolis, R. (2021). *U.S. Solar Photovoltaic System and Energy Storage Cost Benchmarks: Q1 2021*. www.nrel.gov/publications.

Ramasamy, V., & Margolis, R. (2021). *Floating Photovoltaic System Cost Benchmark: Q1 2021 Installations on Artificial Water Bodies*. www.nrel.gov/publications.

Romare, M., & Dahllöf, L. (2017). *The Life Cycle Energy Consumption and Greenhouse Gas Emissions from Lithium-Ion Batteries A Study with Focus on Current Technology and Batteries for light-duty vehicles*. www.ivl.se

Sachenko, A., Kostylyov, V., Sokolovskyi, I., & Evstigneev, M. (2020). Effect of Temperature on Limit Photoconversion Efficiency in Silicon Solar Cells. *IEEE Journal of Photovoltaics*, *10*(1), 63–69. https://doi.org/10.1109/JPHOTOV.2019.2949418

Sahu, A., Yadav, N., & Sudhakar, K. (2016). Floating photovoltaic power plant: A review. In *Renewable and Sustainable Energy Reviews* (Vol. 66, pp. 815–824). Elsevier Ltd. https://doi.org/10.1016/j.rser.2016.08.051

Schwingshackl, C., Petitta, M., Wagner, J. E., Belluardo, G., Moser, D., Castelli, M., Zebisch, M., & Tetzlaff, A. (2013). Wind effect on PV module temperature: Analysis of different

techniques for an accurate estimation. *Energy Procedia*, *40*, 77–86. https://doi.org/10.1016/j.egypro.2013.08.010

Shaner, M. R., Atwater, H. A., Lewis, N. S., & McFarland, E. W. (2016). A comparative technoeconomic analysis of renewable hydrogen production using solar energy. *Energy and Environmental Science*, *9*(7), 2354–2371. https://doi.org/10.1039/c5ee02573g

Shiva Kumar, S., & Lim, H. (2022). An overview of water electrolysis technologies for green hydrogen production. In *Energy Reports* (Vol. 8, pp. 13793–13813). Elsevier Ltd. https://doi.org/10.1016/j.egyr.2022.10.127

Short, W., Packey, D. J., & Holt, T. (1995). *A Manual for the Economic Evaluation of Energy Efficiency and Renewable Energy Technologies*.

Singlitico, A., Østergaard, J., & Chatzivasileiadis, S. (2021). Onshore, offshore or in-turbine electrolysis? Techno-economic overview of alternative integration designs for green hydrogen production into Offshore Wind Power Hubs. *Renewable and Sustainable Energy Transition*, *1*, 100005. https://doi.org/10.1016/j.rset.2021.100005

Skoplaki, E., & Palyvos, J. A. (2009). On the temperature dependence of photovoltaic module electrical performance: A review of efficiency/power correlations. *Solar Energy*, *83*(5), 614–624. https://doi.org/10.1016/j.solener.2008.10.008

Squadrito, G., Agatino, N., & Gaetano, M. (2018). *Oxygen from electrolysis for medical use: an economically feasible route*.

Steffen, B. (2020). Estimating the cost of capital for renewable energy projects. *Energy Economics*, *88*. https://doi.org/10.1016/j.eneco.2020.104783

Stehly, T., & Duffy, P. (2020). *2020 Cost of Wind Energy Review*. www.nrel.gov/publications.

Terlouw, T., Bauer, C., McKenna, R., & Mazzotti, M. (2022). Large-scale hydrogen production via water electrolysis: a techno-economic and environmental assessment. *Energy and Environmental Science*, *15*(9), 3583–3602. https://doi.org/10.1039/d2ee01023b

The Engineering ToolBox. (2004). *Evaporation from a Water Surface*. https://www.engineeringtoolbox.com/evaporation-water-surface-d_690.html

Tsotridis, G., & Pilenga, A. (2021). *EU harmonised protocols for testing of low temperature water electrolysers*. https://doi.org/10.2760/58880

UNFCCC. (2016). *THE PARIS AGREEMENT*. https://treaties.un.org/Pages/ViewDetails.aspx?src=TREATY&mtdsg_no=XXVII-7-

Vestas. (2023). *2 MW platform*. https://nozebra.ipapercms.dk/Vestas/Communication/Productbrochure/2MWTurbineBrochure/2mw-platform-brochure/?page=10

Vincent Knop. (2022, January 10). *A World Of Energy - LCA of alkaline electrolysers*. http://www.awoe.net/Water-Electrolysis-Alkaline-LCA.html

Wang, F., Franco-Penya, H. H., Kelleher, J. D., Pugh, J., & Ross, R. (2017). An analysis of the application of simplified silhouette to the evaluation of k-means clustering validity. *Lecture Notes in Computer Science (Including Subseries Lecture Notes in Artificial Intelligence and Lecture Notes in Bioinformatics), 10358 LNAI*, 291–305. https://doi.org/10.1007/978-3-319-62416-7_21

Williams, N. R. (1949). *The Calculation of Air Density in Various Units ** (Vol. 30, Issue 9).

Woods, P., Bustamante, H., & Aguey-Zinsou, K.-F. (2022). The hydrogen economy - Where is the water? *Energy Nexus*, *7*, 100123. https://doi.org/10.1016/j.nexus.2022.100123

Yadav, N., Gupta, M., & Sudhakar, K. (2017). Energy assessment of floating photovoltaic system. *International Conference on Electrical Power and Energy Systems, ICEPES 2016*, 264–269. https://doi.org/10.1109/ICEPES.2016.7915941

EMILIANO, B. (2017, September 13). *Netherlands' first floating PV plant is under construction – pv magazine International*. Pv Magazine. https://www.pv-magazine.com/2017/09/13/netherlands-first-floating-pv-plant-is-under-construction/

Google Earth. (2023, October 6). *Google Earth* [Map]. Google Earth. https://earth.google.com/web/@6.28766014,-0.21778763,507.77174589a,161.96348825d,35y,-0h,0t,0r/data=OgMKATA

Stefan, P., & Iain, S. (2023, October 6). *Renewables.ninja*. Renewable.Ninja. https://www.renewables.ninja/

VOLTA RIVER AUTHORITY. (2006). *Akosombo_Daily_Downstream_Elevations_1967_2012* [Dataset; Application/vnd.ms-excel].

VOLTA RIVER AUTHORITY. (2015). *Akosombo Daily Upstream Elevations 1965—2012* [Dataset; Application/vnd.openxmlformats-officedocument.spreadsheetml.sheet].

VOLTA RIVER AUTHORITY. (2017). *AKOSOMBO DAILY PLANT DISCHARGE 1965-2012* [Dataset; Application/vnd.openxmlformats-officedocument.spreadsheetml.sheet].

Appendix

Appendix 1: Sensitivity variables and values

Components	Variables	Values		
		Worst	Base	Good
Floating PV	Lifetime [years]	25	30	35
	TIC [€/kWp]	+10%	TIC	-10%
	Efficiency [%]	-10%	19.9	+10%
Ground PV	Lifetime [years]	20, 25	30	---
	TIC [€/kWp]	+10%	TIC	-10%
	Efficiency [%]	-10%	19.9	+10%
Wind turbines	Lifetime [years]	20	25	30
	TIC [€/kWp]	+10%	0 %	-10%
Electrolysers	Lifetime	-10%	L	+10%
	TIC [€/kW]	+10%	TIC	-10%
	Nominal discount rate	10%	7.4%	4%

Appendix 2: Optimization results of PV systems (Sizes, Electricity and hydrogen produced)

Energy systems	$L_{PV}A$	$L_{PV}P$	$L_{PV}S$	$F_{PV}A$	$F_{PV}P$	$F_{PV}S$
PV [MW]	439	487.6	379.6	513.8	571.4	435.1
Electrolyser [MW]	93.85	104.6	76.23	92.45	102.6	77.44
Battery storage [kWh]	3.055	3.055	3.056	0	0	0
H_2 storage [kgH_2]	794.8	794.8	1057	990.2	1018	1018
H2O compressor [kgH_2/h]	1918	1918	1853	1889	1882	1882
Ultrapure water purification system [m^3/h]	17.12	17.12	16.54	16.86	16.8	16.8
H2O pumping-piping system [m^3/h]	11.17	11.17	11.18	---	---	---
Water storage [m^3]	202.5	202.5	202.5	---	---	---
Total electricity produced [GWh]	593.42	659.06	513.07	726	807.25	614.743
Electricity injected to grid [GWh]	318.01	353.2	280.045	450.17	501	381.14
O2 produced [tons]	43210.9	43210.9	43228.596	43272.3	43277.65	43336.15
Total annualised costs (TACs) [M€]	51.73	62.893	56.59	61.81	74	65.1

Appendix 3 Optimization results of hybrid PV-Wind systems (Sizes, Electricity and hydrogen produced)

Energy systems	**L_{PV}WA**	**L_{PV}WP**	**L_{PV}WS**	**F_{PV}WA**	**F_{PV}WP**	**F_{PV}WS**
PV [MW]	360	399.8	315.7	474.5	531.7	408.4
Wind [MW]	147.7	164	124.9	68	75.52	57.51
Electrolyser [MW]	83.75	93.31	68	90.7	98.52	73.31
Battery storage [kWh]	0	0	0	0	0	0
H2 storage [kgH_2]	387.3	387.3	391.5	1185	1177	1174
H2 compressor [kgH_2/h]	1711	1711	1653	1853	1807	1782
Ultrapure water purification system [m^3/h]	15.28	15.28	14.76	16.55	16.13	15.91
H2O pumping-piping system [m^3/h]	8.734	8.734	8.387	---	---	---
H2O storage [m^3]	202.5	202.5	202.5	---	---	---
Total electricity produced PV [GWh]	486.663	540.5	426.7	670.37	751.24	577.04
Total electricity produced Wind [GWh]	75.241	83.56	63.64	72.89	80.952	61.647
Electricity injected to grid [GWh]	286.71	318.44	257.6	467.383	525.942	405.34
Oxygen produced [tons]	43177.28	43174.1	43178.01	43283.964	43264.35	43289.53
Total annualised costs [M€]	66.33	79.98	75.64	68.7	82.97	78.76

Appendix 4: Wind turbine characteristics

Characteristics	**Values**		**Values**
Rated power	2000 kW	**Swept area**	7,854 m^2
Cut-in wind speed	3 m/s	**Optimal wind speed** (Josué, 2013)	9 m/s
Cut-out wind speed	22 m/s	**Hub height**	90m
Rotor diameter	100 m		